nagra.

Arbeitsbericht NAB 21-21

TBO Bözberg-1-1: Data Report

Dossier VI Wireline Logging, Micro-hydraulic Fracturing and Pressure-meter Testing

February 2022

J. Gonus, E. Bailey, J. Desroches &
R. Garrard

National Cooperative
for the Disposal of
Radioactive Waste

Hardstrasse 73
P.O. Box 280
5430 Wettingen
Switzerland
Tel. +41 56 437 11 11

www.nagra.ch

nagra.

Arbeitsbericht NAB 21-21

TBO Bözberg-1-1: Data Report

Dossier VI Wireline Logging, Micro-hydraulic Fracturing and Pressure-meter Testing

February 2022

J. Gonus[1], E. Bailey[1], J. Desroches[1] & R. Garrard[2]

[1] Ad Terra Energy
[2] Nagra

Keywords:
BOZ1-1, Jura Ost, TBO, deep drilling campaign, wireline logging, petrophysical logging, in-situ testing, micro-hydraulic fracturing, pressure-meter testing

National Cooperative for the Disposal of Radioactive Waste

Hardstrasse 73
P.O. Box 280
5430 Wettingen
Switzerland
Tel. +41 56 437 11 11

www.nagra.ch

Nagra Arbeitsberichte ("Working Reports") present the results of work in progress that have not necessarily been subject to a comprehensive review. They are intended to provide rapid dissemination of current information.

This NAB aims at reporting drilling results at an early stage. Additional borehole-specific data will be published elsewhere.

In the event of inconsistencies between dossiers of this NAB, the dossier addressing the specific topic takes priority. In the event of discrepancies between Nagra reports, the chronologically later report is generally considered to be correct. Data sets and interpretations laid out in this NAB may be revised in subsequent reports. The reasoning leading to these revisions will be detailed there.

This Dossier was prepared by a project team consisting of:
J. Gonus (petrophysics QC, theoretical concepts and log analysis)
E. Bailey (introductory chapters, BHI QC and project management)
J. Desroches (MHF QC and theoretical concepts)
R. Garrard (coordination and QC review)

Editorial work: P. Blaser and M. Unger

Petrophysical log graphic files were created using Geolog Emerson E&P Software - Emerson Paradigm and Terrastation.

The Dossier has greatly benefitted from reviews by external and internal experts. Their input and work are very much appreciated.

List of Contents

List of Tables

List of Figures

List of Appendices

Note: Only in the digital version of this report Appendices A – F can be found under the paper clip symbol.

1 Introduction

1.1 Context

To provide input for site selection and the safety case for deep geological repositories for radioactive waste, Nagra has drilled a series of deep boreholes ("Tiefbohrungen", TBO) in Northern Switzerland. The aim of the drilling campaign is to characterise the deep underground of the three remaining siting regions located at the edge of the Northern Alpine Molasse Basin (Fig. 1-1).

In this report, we present the results from the Bözberg-1-1 borehole.

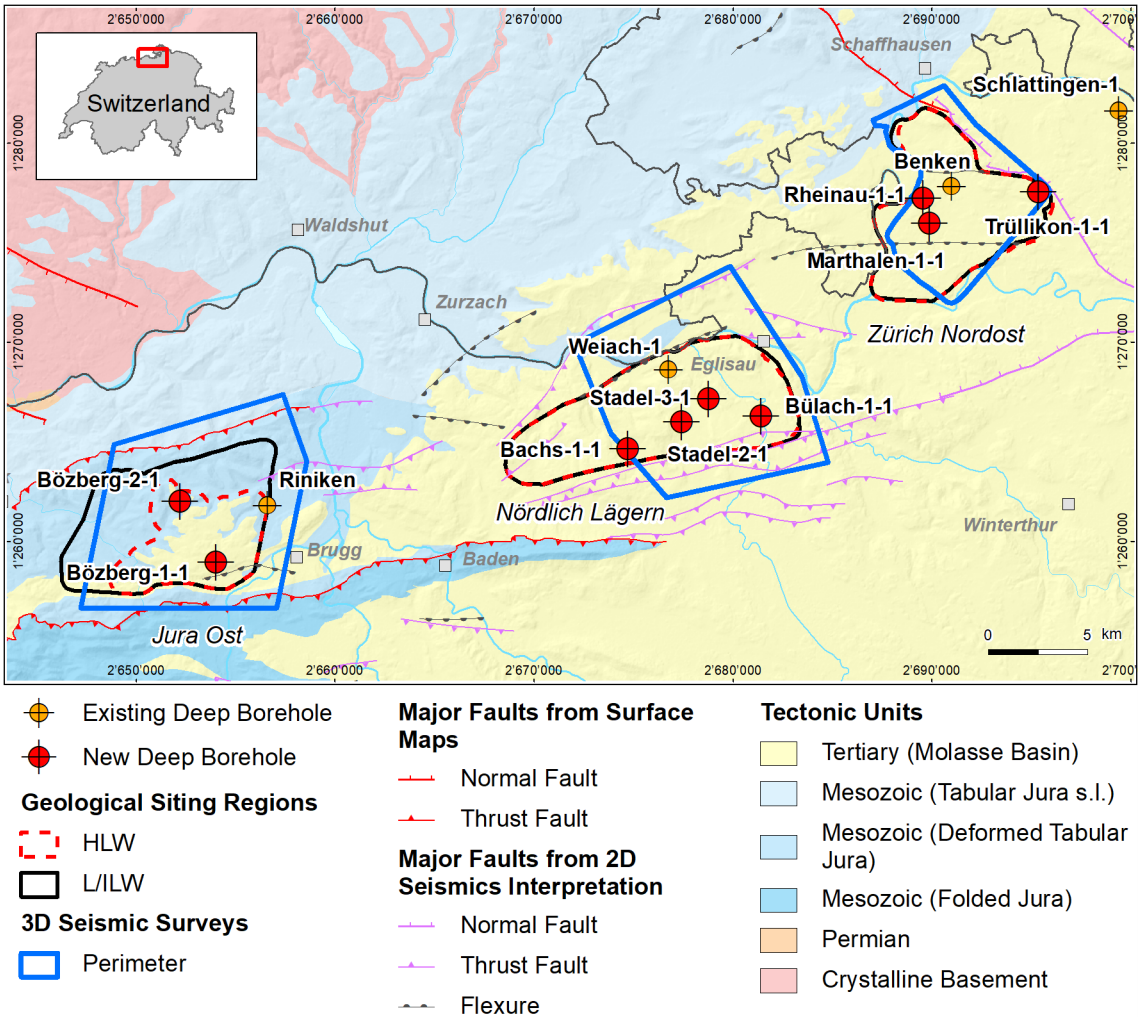

Fig. 1-1: Tectonic overview map with the three siting regions under investigation

1.2 Location and specifications of the borehole

The Bözberg-1-1 (BOZ1-1) exploratory borehole is the fourth borehole drilled within the framework of the TBO project. The drill site is located in the southern part of the Jura Ost siting region (Fig. 1-2). The borehole specifications are provided in Tab. 1-1.

Due to a lost packer system, the borehole was cemented up to 682 m MD[1] (*cf.* Dossier I). Resuming coring operations, a sidetrack was initiated with a kickoff point (KOP) at 709 m MD. This sidetrack was labelled Bözberg-1-1B (BOZ1-1B). BOZ1-1B reached a final depth of 1'037.39 m MD. For easier communication and labelling, the name BOZ1-1 is generally used for this borehole, including the sidetrack, unless stated otherwise.

Tab. 1-1: General information about the BOZ1-1 borehole

Siting region	Jura Ost
Municipality	Bözberg (Canton Aargau / AG), Switzerland
Drill site	Bözberg-1 (BOZ1)
Borehole	Bözberg-1-1 (BOZ1-1) including sidetrack Bözberg-1-1B (BOZ1-1B)
Coordinates	LV95: 2'653'995.815 / 1'258'925.446
Elevation	Ground level = top of rig cellar: 513.29 m above sea level (asl)
Borehole depth	1'037.39 m measured depth (MD) below ground level (bgl) for BOZ1-1B
Drilling period	27th April 2020 – 2nd December 2020 (spud date to end of rig release)
Drilling company	PR Marriott Drilling Ltd
Drilling rig	Rig-16 Drillmec HH102
Drilling fluid	Water-based mud with various amounts of different components such as[2]: 0 – 250 m: Polymers 250 – 882 m: Potassium silicate & polymers 882 – 1'037.39 m: Sodium chloride & polymers

The lithostratigraphic profile and the casing scheme are shown in Fig. 1-3. The comparison of the core versus log depth[3] of the main lithostratigraphic boundaries in the BOZ1-1 borehole is shown in Tab. 1-2.

[1] Measured depth (MD) refers to the position along the borehole trajectory, starting at ground level, which for this borehole is the top of the rig cellar. For a perfectly vertical borehole, MD below ground level (bgl) and true vertical depth (TVD) are the same. In all Dossiers depth refers to MD unless stated otherwise.

[2] For detailed information see Dossier I.

[3] Core depth refers to the depth marked on the drill cores. Log depth results from the depth observed during geophysical wireline logging. Note that the petrophysical logs have not been shifted to core depth, hence log depth differs from core depth.

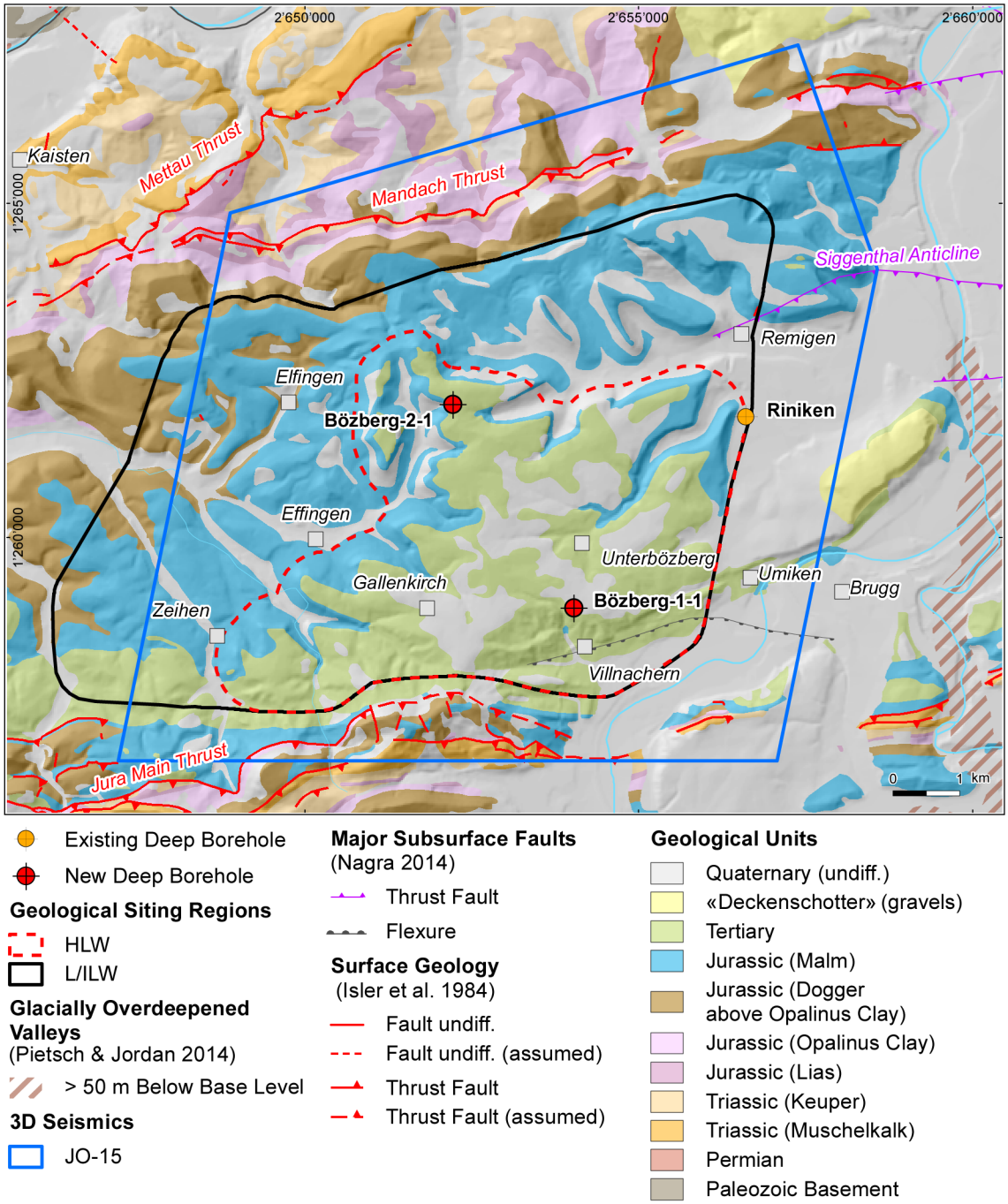

Fig. 1-2: Overview map of the investigation area in the Jura Ost siting region with the location of the BOZ1-1 borehole in relation to the boreholes Riniken and BOZ2-1

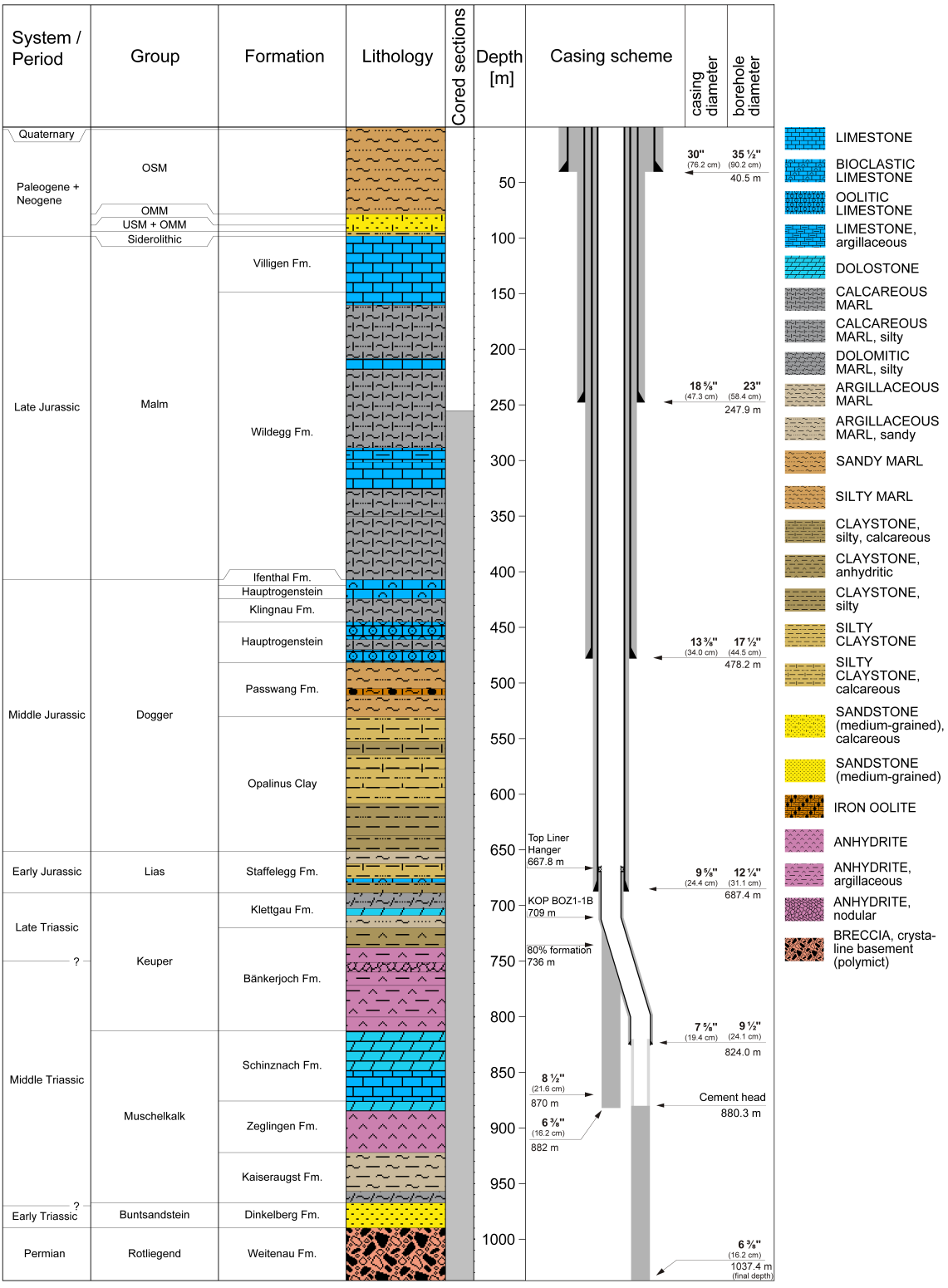

Fig. 1-3: Lithostratigraphic profile and casing scheme for the BOZ1-1 borehole[4]

[4] For detailed information see Dossier I and III.

Tab. 1-2: Core and log depth for the main lithostratigraphic boundaries in the BOZ1-1 borehole[5]

System / Period	Group	Formation	Core depth in m (MD)	Log depth in m (MD)	
Quaternary			**2**		—
Paleogene + Neogene	OSM		78		—
	OMM		88		—
	USM / OMM		94		—
	Siderolithic		**98**		—
Jurassic	Malm	Villigen Formation	148		—
		Wildegg Formation	406.67	406.72	—
	Dogger	Ifenthal Formation	411.91	411.94	—
		Hauptrogenstein	424.11	424.13	—
		Klingnau Formation	444.85	444.93	—
		Hauptrogenstein	481.50	481.55	—
		Passwang Formation	530.28	530.32	—
		Opalinus Clay	651.39	651.46	—
	Lias	Staffelegg Formation	**688.72**	**688.76**	—
Triassic	Keuper	Klettgau Formation	720.03	720.21	—
		Bänkerjoch Formation	812.62	812.45	—
	Muschelkalk	Schinznach Formation	875.89	876.05	—
		Zeglingen Formation	922.22	922.30	—
		Kaiseraugst Formation	967.38	967.70	—
	Buntsandstein	Dinkelberg Formation	**989.89**	**989.83**	—
Permian	Rotliegend	Weitenau Formation	1037.39 final depth		

[5] For details regarding lithostratigraphic boundaries see Dossier III and IV; for details about depth shifts (core goniometry) see Dossier V.

1.3 Documentation structure for the BOZ1-1 borehole

NAB 21-21 documents the majority of the investigations carried out in the BOZ1-1 borehole, including laboratory investigations on core material. The NAB comprises a series of stand-alone dossiers addressing individual topics and a final dossier with a summary composite plot (Tab. 1-3).

This documentation aims at early publication of the data collected in the BOZ1-1 borehole. It includes most of the data available approximately one year after completion of the borehole. Some analyses are still ongoing (e.g. diffusion experiments, analysis of veins, hydrochemical interpretation of water samples) and results will be published in separate reports.

The current borehole report will provide an important basis for the integration of datasets from different boreholes. The integration and interpretation of the results in the wider geological context will be documented later in separate geoscientific reports.

Tab. 1-3: List of dossiers included in NAB 21-21

Black indicates the dossier at hand.

Dossier	Title	Authors
I	TBO Bözberg-1-1: Drilling	M. Ammen, P.-J. Palten, J. Vliek, K. Gollob & K. Hilgendorf
II	TBO Bözberg-1-1: Core Photography	D. Kaehr & M. Gysi
III	TBO Bözberg-1-1: Lithostratigraphy	M. Schwarz, P. Schürch, H. Naef, P. Jordan, R. Felber, T. Ibele & M. Gysi
IV	TBO Bözberg-1-1: Microfacies, Bio- and Chemostratigraphic Analyses	S. Wohlwend, H.R. Bläsi, S. Feist-Burkhardt, B. Hostettler, U. Menkveld-Gfeller, V. Dietze & G. Deplazes
V	TBO Bözberg-1-1: Structural Geology	A. Ebert, L. Gregorczyk, S. Cioldi, E. Hägerstedt, & M. Gysi
VI	TBO Bözberg-1-1: Wireline Logging, Micro-hydraulic Fracturing and Pressure-meter Testing	J. Gonus, E. Bailey, J. Desroches & R. Garrard
VII	TBO Bözberg-1-1: Hydraulic Packer Testing	R. Schwarz, R. Beauheim, S.M.L. Hardie, M. Voß & A. Pechstein
VIII	TBO Bözberg-1-1: Rock Properties, Porewater Characterisation and Natural Tracer Profiles	P. Wersin, L. Aschwanden, L. Camesi, E.C. Gaucher, T. Gimmi, A. Jenni, M. Kiczka, U. Mäder, M. Mazurek, D. Rufer, H.N. Waber, C. Zwahlen & D. Traber
IX	TBO Bözberg-1-1: Rock-mechanical and Geomechanical Laboratory Testing	E. Crisci, L. Laloui & S. Giger
X	TBO Bözberg-1-1: Petrophysical Log Analysis	S. Marnat & J.K. Becker
	TBO Bözberg-1-1: Summary Plot	Nagra

1.4 Scope and objectives of this dossier

The dossier at hand describes the acquisition, quality control and results of the Petrophysical Logging (PL), Micro-hydraulic Fracturing (MHF) and Pressure-meter Testing (PMT) wireline logging measurements performed in the BOZ1-1 borehole.

Petrophysical log measurements were acquired in open borehole conditions (no casing) with wire-line conveyed logging tools to determine continuous profiles across the borehole of physical and chemical properties of the formation, including its mineralogy, clay types, porosity, fluid content, and acoustic properties. Petrophysical logs were further acquired to obtain high-resolution circumferential images of the borehole wall, as well as to measure borehole physical parameters such as its geometry, mud resistivity and mud temperature. In addition to the open hole logs, temperature logs were acquired post-completion to measure the undisturbed mud temperature.

A series of in situ stress measurements were performed using the micro-hydraulic fracturing technique to estimate the orientation and magnitude of the earth stress at different depths. The objectives of the MHF testing programme were to provide estimates of the in situ stress state in the Opalinus Clay potential host rock and adjacent rock formations and to provide calibration points for mechanical earth models (MEM) of the rock mass (both 1D and 3D).

Pressure-meter testing was performed at the same time as MHF testing using the same module that was used to perform sleeve fracturing and sleeve reopening during MHF operations. As this was a new application of the tool, the primary objectives of the PMT were to explore the best tool string combination and protocol to obtain an interpretable pressure record from which the in situ shear modulus of the formation can be estimated. PMT results can then be used for comparison with future dilatometer tests which will be performed in the Stadel-3-1 (STA3-1) and Stadel-2-1 (STA2-1) boreholes.

All PL, MHF and PMT testing were performed by the wireline logging company Schlumberger (SLB). Ad Terra Energy (formerly Geneva Petroleum Consultants International) were responsible for planning wireline operations, technical supervision at the worksite, quality assurance and control (QA-QC) of data, database management and general wireline logging support.

This dossier is organised as follows:

- Chapter 2: The sequence of events for PL, MHF and PMT testing operations, and associated log / data coverage is provided.
- Chapter 3: The QA-QC procedure used to assess the quality of the petrophysical logs is detailed. A continuous profile of each log across the entire measured depth of the borehole is quality-controlled, corrected and spliced together to generate a quality-controlled composite log. The results of the composite log are discussed. The composite log will then be used as the final log data for input into further data analysis processes such as formation evaluation (e.g. Stochastic Petrophysical Log Analysis described in Dossier X), calibration with seismic data and integration with sedimentology and structural geology data (from cores, cuttings, adjacent boreholes and regional geology).
- Chapter 4: Although Borehole Imagery (BHI) logs were acquired as part of the petrophysical logging, the objectives of BHI are related to both Structural Geology (analysis of image features described in Dossier V) and MHF / PMT (firstly the selection of stations for stress measurements, then the analysis of fractures induced by tests). Thus, the QC, processing and interpretation processes of BHI are described in a chapter separate from the QA-QC procedures of the other petrophysical logs in Chapter 3.

- Chapter 5: MHF test procedures and preliminary results are presented.
- Chapter 6: PMT procedures and preliminary results are presented.
- Finally, this report includes a set of appendices, where spliced PL, pre- and post-MHF / PMT borehole images and MHF / PMT data can be found.

2 Wireline logging and testing operations

The BOZ1-1 borehole was planned in 5 drilling sections (also commonly referred to as phases). After installation of the 30" outer diameter (OD) standpipe, Section I was drilled with the 23" drill bit for installation of the 18⅝" OD casing. Sections II through IV were continuously cored and logged in 6⅜", before reaming (opening up) to 8½" for MHF and PMT testing. After wireline logging operations in Sections II and III were completed, the borehole was reamed to 17½" and 12¼" to accommodate the OD 13⅜" casing and 9⅝" casings, respectively. While coring Section IV, mud losses were experienced, and part of the packer assembly was lost and could not be retrieved. As a consequence, the interval from 682 m to 853 m MD was cemented with two plugs: 1) a fibrous, light cement (1.36 specific gravity [SG]) was used from 777.2 m to 853 m MD to plug the zone where losses were experienced; 2) a denser cement (1.75 SG) with higher compressive strength was used from 682 m to 769 m MD to enable the side-track to be drilled. The kick-off point (KOP) of the BOZ1-1B borehole was 709 m MD. The side-track was then opened up to 9⅞" for installation of the 7⅝" liner. Section V was subsequently cored in 6⅜" and logged / tested. Once open borehole logging / testing operations were completed, the borehole was backfilled with cement up to 880.25 m MD, leaving the Schinznach Formation exposed for installation of a long-term monitoring system. One post-completion, petrophysical log was acquired to measure the undisturbed mud temperature. Detailed descriptions of the borehole design and mud conditions at the time of logging and testing are included in the Excel Composite Report (Appendix A), under the worksheets entitled 'Borehole design' and 'Hole & mud system'. Additional details about borehole configuration, casing and cementing scheme and mud parameters can be found in Dossier I.

Wireline logging and testing operations were divided into the following groups of activities:

- Petrophysical Logging (PL)
- Micro-hydraulic Fracturing (MHF)
- Pressure-meter Testing (PMT)
- *Technical Logging (TL)*
- *Vertical Seismic Profiling (VSP)*

Petrophysical logs are continuous measurements (recorded every half foot or approximately 15 cm) of mineralogy and physical properties of formation rocks, their contained fluids, and the borehole environment between the wireline conveyed logging tool sensors and the borehole wall. Petrophysical logs were acquired with conventional and advanced wireline-conveyed logging tools. Conventional tools measured Depth (measured depth [MD], or log depth, that is the depth reference for all wireline measurements), Total Gamma Ray (naturally occurring gamma radiation), Spontaneous Potential (electric potential difference between the formation and an electrode at surface), Temperature, Caliper (measurement of the borehole diameter), Inclinometer (measurement of the borehole trajectory), as well as the standard "quad combo" tools: Resistivity (electrical resistivity at different depths of investigation in the formation), Sonic (compressional and shear wave slowness), Density (measurement of the bulk density and the photoelectric factor), and Neutron (measurement of the neutron hydrogen index, a proxy of porosity, as well as the sigma capture cross-section). Advanced tools measured the Spectral Gamma Ray (potassium, thorium and uranium contributions to the total naturally occurring gamma radiation), Elemental Spectroscopy, and Microresistivity and Ultrasonic borehole images. These logging tools and their main measurements are described in detail in the subsequent Chapter 3 – Petrophysical Logging and Chapter 4 – Borehole Imagery.

MHF involves using wireline-conveyed testing equipment to initiate and analyse the characteristics of micro-hydraulic fractures through several opening / closure cycles, to estimate the current stress state in the rock formation at the 1 m scale. Tests were conducted using the SLB Modular Formation Dynamics Tester (MDT), which uses packer modules, surface-controlled downhole valves, downhole pressure gauges and a downhole pump to initiate and propagate fractures at predefined discrete depths. MHF tests are described in Chapter 5 – Micro-hydraulic Fracturing.

PMT was conducted using the single packer module from the MDT tool that is used to perform sleeve fracturing and reopening operations during MHF testing. Different packer types, pump types and protocols were tested to find the optimum toolstring and methodology for obtaining an interpretable pressure record in the formation of interest. At least one PMT test was performed in each section where MHF tests were conducted. PMT tests are described in Chapter 6 – Pressuremeter Testing.

As well as PL and MHF / PMT operations, wireline operations also included Technical Logging (TL) and Vertical Seismic Profiling (VSP). TL acquired data on the physical properties of the open borehole (geometry and trajectory) and the permanent casing installation. The borehole geometry was measured using calipers for both assessing the borehole condition (breakouts / washouts present) and determining the volume of cement needed for casing installations. The borehole inclination and azimuth were measured to confirm the borehole verticality and identify its trajectory. To assess the quality of the cement behind the casing, Cement Bond Logs (CBL) and acoustic impedance logs were acquired using sonic (MSIP) and ultrasonic imaging (USIT) tools. Borehole deviation surveys, cement volume calculations and CBL logs are described in Dossier I. VSP acquired high resolution borehole seismic measurements used for correlation with, and enhancement of, surface seismic data. VSP will be addressed in a separate document. TL and VSP are not described further in this report.

A summary of all wireline logging and testing activities carried out in the BOZ1-1 borehole is given in Tab. 2-1. Fig. 2-1 depicts graphically the log coverage for the PL, MHF / PMT campaigns. In total, 7 PL and 4 MHF / PMT campaigns were undertaken. Open hole PL and MHF / PMT was conducted in Sections II to V of BOZ1-1. A more detailed analysis of the log measurement coverage is provided in Chapter 3.

Details of the logging runs, logging dates, wireline logging company, logging interval, logging suite and principal measurements acquired for PL and MHF / PMT operations are provided in Tab. 2-2. Mnemonics for each tool in the logging suite listed in this table are given in Tab. 2-3.

Tab. 2-1: Logging and testing activities during drilling of the BOZ1-1 borehole

Drilling phase / section	**Permanent casing size** **Casing / liner shoe depth**	**Open hole interval and bit size**	**Start date**	**End date**	**Coring**	**Technical Logging**	**Petrophysical Logging**	**Micro-hydraulic Fracturing / Pressure-meter Testing**	**Vertical Seismic Profiling**
I	18⅝" 0 to 247.9 m	247.9 to 251 m in 17½"	27.04.2020	10.05.2020		×			
II	18⅝" 0 to 247.9 m	247.9 to 251 m in 17½" 251 to 255 m in 8½" 255 to 480 m 6⅜"	10.05.2020	27.06.2020	×	×	×		
		247.9 to 251 m in 17½" 251 to 255 m in 12¼" 255 to 480 m in 8½"					×	×	
	13⅜" 0 to 478.2 m	478.2 to 481 m in 12¼"				×			
III	13⅜" 0 to 478.2 m	478.2 to 481 m in 12¼" 481 to 483 m in 8½" 483 to 564 m in 6⅜"	27.06.2020	31.08.2020	×		×		
		478.2 to 481 m in 12¼" 481 to 483 m in 8½" 483 to 690 m in 6⅜"			×		×		
		478.2 to 481 m in 12¼" 481 to 690 m in 8½"					×	×	
		478.2 to 689.1 m in 12¼" 689.1 to 690 m in 8½"				×			×
IV	9⅝" 0 to 687.4 m	687.4 to 870 m in 8½" 870 to 882 m in 6⅜"	31.08.2020	07.11.2020	×	×	×	×	
V	7⅝" 667.8 to 824.0 m	824 to 825 m in 9⅝" 825 to 1'037.39 m in 6⅜"	07.11.2020	02.12.2020	×	×	×	×	×

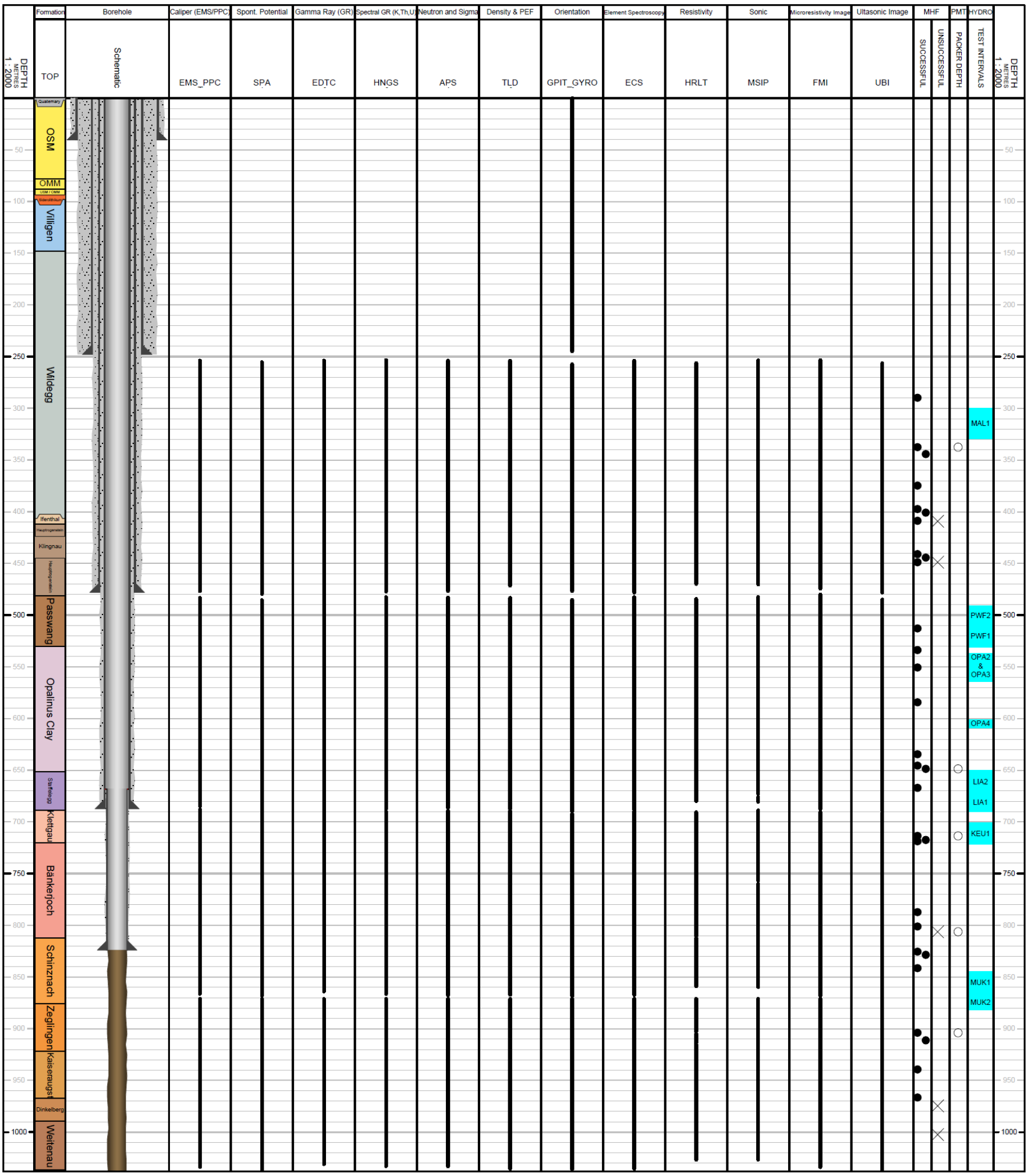

Fig. 2-1: Petrophysical log and MHF / PMT testing coverage at BOZ1-1 (scale of 1:2'000)

Tab. 2-2: Logging and testing sequence of events (only PL, MHF and PMT)

Phase / Section	Run	Operation	Logging date	Contractor	Logging interval [m MD]	Logging suite (see list of abbreviations)	Measurements																Remarks
							Gamma ray	Resistivity	Microresistivity	Density	Sonic	Neutron hydrogen index	Sigma capture cross-section	Photoelectric factor	Spontaneous potential	Borehole imaging	Caliper	Spectral gamma ray	Elemental spectroscopy	Inclinometer	Temperature	MHF / PMT	
II	2.1.1	PL	25.05.2020	SLB	256.2 to 478.2	FMI-EMS-EDTC-LEH.QT	×									×	×			×	×		GR reference for Section I and subsequent runs
	2.1.2		25.05.2020	SLB	253.8 to 476.5	APS-TLD-MCFL-EDTC-LEH.QT	×		×	×		×	×	×			×						
	2.1.3		25.05.2020	SLB	253.8 to 478.2	ECS-EDTC-LEH.QT	×												×				
	2.1.4		25. – 26.05.2020	SLB	241.9 to 478.4	HNGS-EMS-EDTC-LEH.QT	×										×	×			×		
	2.1.5		26.05.2020	SLB	231.7 to 478.2	PPC-MSIP-PPC-GPIT-EDTC-LEH.QT	×				×						×			×			
	2.1.6		26.05.2020	SLB	243.7 to 481.3	SP-EMS-HRLT-EDTC-LEH.QT	×	×							×		×				×		
	2.3.1	PL	04.06.2020	SLB	n/a	EMS-EDTC-LEH.QT	×										×				×		Run aborted because tools could not pass the rathole below 18⅝" casing shoe – washouts up to 26"
	2.3.2		04.06.2020	SLB	478.4 to 226.4	BNS-EMS-EDTC-LEH.QT	×										×				×		Bottom nose (BNS) added due to problems passing rathole – successful descent
	2.3.3		04. – 05.06.2020	SLB	474.5 to 253.5	UBI-GPIT-EDTC-LEH.QT	×									×				×			

Tab. 2-2: continued

Phase / Section	Run	Operation	Logging date	Contractor	Logging interval [m MD]	Logging suite (see list of abbreviations)	Measurements																Remarks
							Gamma ray	Resistivity	Microresistivity	Density	Sonic	Neutron hydrogen index	Sigma capture cross-section	Photoelectric factor	Spontaneous potential	Borehole imaging	Caliper	Spectral gamma ray	Elemental spectroscopy	Inclinometer	Temperature	MHF / PMT	
II continued	2.3.4	MHF	05.06.2020	SLB	n/a	MRPA(dual)- MRPA(single)- MRSC(exit)- MRSC(exit)- MRPO(HP)-5×MRSC(water)- MRSC(exit)- MRPC-EDTC-LEH.QT																×	Run aborted because tools could not pass the rathole below 18⅝" casing shoe – decision to "taper" borehole with 12¼" drill bit between 251 and 255 m MD
	2.4.1	PL	05.06.2020	SLB	n/a	EMS-EDTC-LEH.QT	×										×				×		Run to check if tapering of rathole worked; could not pass ledge at 251 m MD – decision to run auxiliary 13⅜" casing to 247 m
	2.5.1		06.06.2020	SLB	n/a	EMS-EDTC-LEH.QT	×										×				×		Toolstring hung up at 251 m, - POOH to install BNS
	2.5.2		06.06.2020	SLB	467.8 to 237.1	BNS-EMS-EDTC-LEH.QT	×										×				×		Successful descent
	2.5.3	MHF	06.06.2020	SLB	n/a	MRPA(dual)-MRPC-EDTC-LEH.QT																×	MDT short string; unsuccessful descent; decision to reposition 13⅜" casing closer to the ledge at 251 m MD
	2.6.1	PL	06.06.2020	SLB	299.0 to 239.3	BNS-EMS-EDTC-LEH.QT	×										×				×		Successful run

Tab. 2-2: continued

Phase / Section	Run	Operation	Logging date	Contractor	Logging interval [m MD]	Logging suite (see list of abbreviations)	Measurements																Remarks
							Gamma ray	Resistivity	Microresistivity	Density	Sonic	Neutron hydrogen index	Sigma capture cross-section	Photoelectric factor	Spontaneous potential	Borehole imaging	Caliper	Spectral gamma ray	Elemental spectroscopy	Inclinometer	Temperature	MHF / PMT	
II continued	2.6.2	PL	06.06.2020	SLB	n/a	MRPA(dual)-MRPC-EDTC-LEH.QT																×	MDT short string; successful descent; POOH to connect the rest of the toolstring
	2.6.3	MHF	06. – 07.06.2020	SLB	3 stations	MRPA(dual)- MRPA(single)- MRSC(exit)-MRSC(exit)- MRPO(HP)-5xMRSC(water)-MRSC(exit)- MRPC-EDTC-LEH.QT																×	2 successful MHF tests out of 3 ; problem with pumpout module (MRPO) which required tool reconfiguration
	2.6.4		07. – 09.06.2020	SLB	5 stations																	×	5 successful MHF tests out of 5: 1 PMT test included in an MHF test
	2.6.5		09.06.2020	SLB	1 station																	×	1 successful MHF test out of 1; 1 dedicated PMT test
	2.6.6	PL	09.06.2020	SLB	255.8 to 459.1	FMI-EMS-EDTC-LEH.QT	×									×	×			×	×		Post-MHF
III	3.1.1	PL	06.07.2020	SLB	484.6 to 563.2	FMI-EMS-EDTC-LEH.QT	×									×	×			×	×		
	3.2.1		28.07.2020	SLB	487.0 to 689.0	FMI-EMS-EDTC-LEH.QT	×									×	×			×	×		
	3.2.2		29.07.2020	SLB	450.0 to 688.2	PPC-MSIP-PPC-GPIT-EMS-EDTC-LEH.QT	×				×						×			×	×		
	3.2.3		29.07.2020	SLB	517.7 to 612.7	TLD-MCFL-EDTC-LEH.QT	×		×	×				×									
	3.2.4		29.07.2020	SLB	502.7 to 606.2	APS-EMS-EDTC-LEH.QT	×					×	×				×				×		

Tab. 2-2: continued

Phase / Section	Run	Operation	Logging date	Contractor	Logging interval [m MD]	Logging suite (see list of abbreviations)	Measurements																Remarks
							Gamma ray	Resistivity	Microresistivity	Density	Sonic	Neutron hydrogen index	Sigma capture cross-section	Photoelectric factor	Spontaneous potential	Borehole imaging	Caliper	Spectral gamma ray	Elemental spectroscopy	Inclinometer	Temperature	MHF / PMT	
III continued	3.2.5	PL	29.07.2020	SLB	465.0 to 688.2	ECS-EDTC-LEH.QT	×												×				
	3.2.6		30.07.2020	SLB	475.0 to 687.2	HNGS-EDTC-LEH.QT	×											×					
	3.2.7		30.07.2020	SLB	468.2 to 692.7	SP-EMS-HRLT-EDTC-LEH.QT	×	×							×		×				×		
	3.3.1	PL	18.08.2020	SLB	450.0 to 688.8	EMS-EDTC-LEH.QT	×										×				×		
	3.3.2		19.08.2020	SLB	474.6 to 687.6	UBI-GPIT-EDTC-LEH.QT	×									×				×			
	3.3.3	MHF	19.08.2020	SLB	7 stations	MRPA(dual)- MRPA(single)- MRSC(exit)- MRSC(exit)- MRPO(HP)-4xMRSC(water)- MRSC(exit)- MRPC-EDTC-LEH.QT																×	7 successful MHF tests out of 7; 1 dedicated PMT test
	3.3.4	PL	22.08.2020	SLB	480.5 to 689.0	FMI-EDTC-LEH.QT	×									×	×			×			Post-MHF
IV	4.3.1	PL	10.10.2020	SLB	691.0 to 869.5	FMI-EMS-EDTC-LEH.QT	×									×	×			×	×		
	4.3.2		10.10.2020	SLB	690.3 to 868.5	UBI-GPIT-EDTC-LEH.QT	×									×				×			
	4.3.3		10.10.2020	SLB	465.1 to 868.2	PPC-MSIP-PPC-GPIT-EDTC-LEH.QT	×				×						×			×			
	4.3.5		11.10.2020	SLB	867.9 to 462.7	TLD-MCFL-EDTC-LEH.QT	×		×	×				×									
	4.3.6		11.10.2020	SLB	867.6 to 688.8	APS-EMS-EDTC.LEH.QT	×					×	×				×				×		
	4.3.7		11.10.2020	SLB	867.7 to 688.0	ECS-EDTC-LEH.QT	×												×				
	4.3.8		12.10.2020	SLB	866.91 to 670.1	HNGS-EDTC-LEH.QT	×											×					
	4.3.9		12.10.2020	SLB	869.4 to 688.2	SP-EMS-HRLT-EDTC-LEH.QT	×	×							×		×				×		
	4.3.10		12.10.2020	SLB	670.1 to 867.6	PPC-PPC-EDTC-LEH.QT	×										×						Run added before wiper trip due to concerns about restriction at 715 m

Tab. 2-2: continued

Phase / Section	Run	Operation	Logging date	Contractor	Logging interval [m MD]	Logging suite (see list of abbreviations)	Measurements																Remarks
							Gamma ray	Resistivity	Microresistivity	Density	Sonic	Neutron hydrogen index	Sigma capture cross-section	Photoelectric factor	Spontaneous potential	Borehole imaging	Caliper	Spectral gamma ray	Elemental spectroscopy	Inclinometer	Temperature	MHF / PMT	
IV continued	4.4.1	PL	13.10.2020	SLB	670.1 to 865.5	PPC-PPC-EDTC-LEH.QT	×										×						Run added after wiper trip to see if restriction was removed
	4.4.2	MHF	13.10.2020	SLB	7 stations	MRPA(dual)-MRPA(single)-MRSC(exit)-MRSC(forced closure)-MRPO(XP)-MRSC(exit)-MRPO(HP)- 4xMRSC(water)-MRSC(exit)-MRPC-EDTA-EDTC-LEH.QT																	×	6 successful MHF tests out of 7; 1 dedicated PMT test, 1 PMT test integrated in an MHF test
	4.4.3	PL	16.10.2020	SLB	690.9 to 866.8	FMI-EDTC-LEH.QT	×									×	×			×			Post-MHF
V	5.1.1	PL	22. – 23.11.2020	SLB	828.2 to 1'036.8	FMI-EMS-EDTC-LEH.QT	×									×	×			×	×		
	5.1.2		23.11.2020	SLB	831.0 to 1'034.0	UBI-GPIT-EDTC-LEH.QT	×									×				×			
	5.1.3		23.11.2020	SLB	810.3 to 1'034.8	PPC-MSIP-PPC-GPIT-EDTC-LEH.QT	×				×						×			×			
	5.1.5		23.11.2020	SLB	810.0 to 1'036.5	TLD-MCFL-EDTC-LEH.QT	×		×	×				×									
	5.1.6		23. – 24.11.2020	SLB	824.0 to 1'034.4	APS-EDTC-LEH.QT	×					×	×				×				×		
	5.1.7		24.11.2020	SLB	824.1 to 1'036.8	ECS-EDTC-LEH.QT	×												×				
	5.1.8		24.11.2020	SLB	802.5 to 1'032.8	HNGS-EDTC-LEH.QT	×											×					
	5.1.9		24.11.2020	SLB	810.2 to 1'037.1	SP-EMS-HRLT-EDTC-LEH.QT	×	×							×		×				×		
	5.1.10	MHF	24. – 25.11.2020	SLB	3 stations	MRPA(dual)- MRPA(single)- MRSC(exit)-2xMRSC(forced closure)- MRPO(XP)-4xMRSC(water)- MRSC(exit)- MRPC-EDTA-EDTC-LEH.QT																	×	3 successful MHF tests out of 3; MDT tool problems which required parts replacements

Tab. 2-2: continued

Phase / Section	**Run**	**Operation**	**Logging date**	**Contractor**	**Logging interval** [m MD]	**Logging suite** (see list of abbreviations)	**Measurements**																**Remarks**
							Gamma ray	**Resistivity**	**Microresistivity**	**Density**	**Sonic**	**Neutron hydrogen index**	**Sigma capture cross-section**	**Photoelectric factor**	**Spontaneous potential**	**Borehole imaging**	**Caliper**	**Spectral gamma ray**	**Elemental spectroscopy**	**Inclinometer**	**Temperature**	**MHF / PMT**	
V continued	5.1.11	MHF	25. – 26.11.2020	SLB	4 stations	MRPA(dual)- MRPA(single)- MRSC(exit)- 2xMRSC(forced closure)- MRPO(XP)- 4xMRSC(water)- MRSC(exit)- MRPC-EDTA-EDTC-LEH.QT																×	3 successful MHF tests out of 4; 1 PMT test (second PMT test was cancelled due to overpull at the end of the run)
	5.1.12	PL	27.11.2020	SLB	1'030.5 to 826.2	FMI-EDTC-LEH.QT	×									×	×			×			
	5.2.1	PL	10.08.2021	SLB	871.0 to 50.0	EMS-EDTC-LEH.QT	×														×		Post completion

Tab. 2-3: Tool mnemonics and measurement details

Logging tool	**Wireline contractor**	**Mnemonic**	**Principal measurement**
APS	SLB	Accelerator porosity sonde	Epithermal and thermal neutrons, sigma capture cross-section of thermal neutrons
ECS	SLB	Elemental capture spectroscopy sonde	Measurement of the relative dry weight element concentration (e.g. Si, Ca, Fe, S, Ti, Gd, Cl and H) and mineralogical model
EDTC	SLB	Enhanced digital telemetry cartridge	Gamma ray measurement of the total natural radioactivity
EMS	SLB	Environmental measurement sonde	6-arm caliper, temperature and mud resistivity
FMI	SLB	Fullbore formation microimager	Microresistivity imaging tool (pad contact)
GPIT	SLB	General purpose inclinometry tool	Orientation/inclination of the borehole
HNGS	SLB	Hostile natural gamma ray sonde	Spectral gamma ray measurements of natural radioactivity (potassium, thorium, uranium)
HRLT	SLB	High resolution laterolog array tool	Laterolog resistivity measurement at different depths of investigation
LEH.QT	SLB	Logging equipment head with tension	Head tension
MCFL	SLB	Microcylindrically focused log	Measures the invaded zone resistivity (Rxo)
MRPA	SLB	Packer modules	Packer modules for stress measurements: - Dual (straddle) for MHF tests - Single for sleeve fracturing, sleeve reopening and PMT tests
MRPO	SLB	Pump out module	Downhole pump for MHF / PMT tests
MRSC	SLB	Sample chamber	Typically used to carry fluid for MHF / PMT tests, usually filled with water. Can also be configured as an exit port.
MSIP	SLB	Modular sonic imaging platform (sonic scanner)	Compressional, shear and Stoneley wave slowness measurements (monopole and dipole sources); cement bond log
PPC	SLB	Power positioning calipers	4-arm caliper that gives dual axis borehole measurements
SP	SLB	Spontaneous potential	Measurement of electrical potential difference between the borehole and the surface
TLD	SLB	Three-detector lithology density	Bulk density and photoelectric absorption factor measurement
UBI	SLB	Ultrasonic borehole imager	High-resolution acoustic (ultrasonic) images of the borehole

3 Petrophysical Logging (PL)

3.1 Petrophysical logging tools and measurements

Below the main petrophysical measurements acquired, and the downhole logging tools deployed are summarised. A detailed description of how the different tools measure the respective parameters and the underlying physics behind these measurements is not the focus of this report. Borehole imaging tools are described in Chapter 4.

- **Borehole deviation / orientation** (GPIT – General Purpose Inclinometry Tool). The GPIT outputs inclinometer measurements. Tool orientation is defined by three parameters: tool deviation, tool azimuth and relative bearing. Borehole trajectory is calculated from the inclinometer measurements. Inclinometer measurements serve to reference the oriented logs (e.g. borehole imagery and sonic dipole logs).
- **Caliper log** (EMS/PPC – Environmental Measurement Sonde/Powered Positioning Caliper). The caliper log uses several coupled pairs of mechanical arms (2 pairs with PPC, 3 pairs with EMS) to continuously measure the borehole shape in different orientations.
- **Density** (TLD – Three-detector Lithology Density). TLD is an induced radiation tool that measures the bulk density of the formation and the photoelectric factor (PEF). It uses a radioactive source to emit gamma photons into the formation. The gamma rays undergo Compton scattering by interacting with the atomic electrons in the formation. Compton scattering reduces the energy of the gamma rays in a stepwise manner and scatters the gamma rays in all directions. When the energy of the gamma rays is less than 0.5 MeV, they can undergo photoelectric absorption by interacting with the electrons. The flux of gamma rays that reach each of the detectors of the TLD is therefore attenuated by the formation, and the amount of attenuation is dependent upon the density of electrons in the formation, which is related to its bulk density. The bulk density of a rock is the sum of the minerals (solids) and fluids volumes (porosity) times their densities. Hence, the formation density tool is key for the determination of porosity, the detection of low-density fluids (gasses) in the pores and mineralogical identification. In addition, the TLD provides the **photoelectric absorption index** (photoelectric factor – PEF), which represents the probability that a gamma photon will be photoelectrically absorbed per electron of the atoms that compose the material. The PEF characterises the mineralogy. The TLD tool is housed in the High-Resolution Mechanical Sonde that also includes the Micro-Cylindrically Focused Log (MCFL) sonde, that measures the **microresistivity** or alternatively, the resistivity very close to the borehole wall (RXOZ). The bulk density was integrated over depth, to provide the overburden pressure or vertical stress (Sv).
- **Element Spectroscopy** (ECS – Elemental Capture Spectroscopy). The ECS is also an induced radiation tool with a radioactive neutron source. The ECS measures the concentration of a series of elements in the formation (Si, Ca, Fe, S, Ti, Gd, Cl, H) by analysing the gamma ray spectrum of back scattered gamma rays. Special processing techniques allow under certain circumstances the measurement of supplementary elements such as Al, Mg, K and Na. The element spectroscopy measurements are provided in dry weight concentrations. SLB uses an algorithm in the field to derive a model of dry weight fractions of minerals from the dry weight element concentrations: clay, clastics (quartz – feldspar – mica, QFM), carbonates, anhydrite / gypsum, salt / evaporite, pyrite, siderite and coal. Advanced models can discriminate limestone and dolomite from carbonates, as well to provide a more quantitative clay measurement. It is important to note that mineralogy model processing is qualitative and should be viewed as an indicator of lithology and not used in any quantitative analysis. Quantitative analysis of the ECS dry weight elements needs to be calibrated against core data.

Dossier X details stochastic processing and interpretation of the ECS dry weight proportions, combined with conventional petrophysical log response, to generate a quantified lithology determination.

- **Gamma Ray** (GR, from the EDTC – Enhanced Digital Telemetry Cartridge). This log measures the total naturally occurring gamma ray radioactivity in the formation rocks (potassium, thorium and uranium are the most common radioactive elements in Earth's crust), which can be used to determine the volume of clay minerals (that contains those elements). The GR log is not valid for clay determination if other minerals contain those elements in significant amounts (e.g. potassic feldspars, organic matter, phosphates). The GR is run with all logging runs because it is used for depth correlation between runs, thanks to its excellent vertical resolution and character. Note this is not to be confused with the Spectral Gamma Ray which is a different tool detailed further below.

- **Neutron Hydrogen Index, commonly named Neutron** (NHI, from the APS – Accelerator Porosity Sonde). A particular accelerator called a Minitron generates high energy neutrons (14 MeV) that are emitted into the formation. Elastic collisions with the atom nuclei slow down the neutrons, a process that is more efficient with nuclei whose mass is close to that of neutron, i.e., hydrogen (the lightest element). Five detectors count the neutrons back from the formation at different distances from the Minitron, allowing for an environmental compensation of the signal. The received signal is mostly (but not only, for example the chlorine atoms bring a significant contribution) dependent on the hydrogen concentration in the formation, hence the Hydrogen Index (HI) measurement: the larger the count, the lower the HI and its uncertainty. The APS tool can measure both an epithermal HI (APLC curve) and a thermal HI (FPLC). The hydrogen content in rocks is mostly in the fluids contained within, generally water or hydrocarbons, which have a HI close to 1 v/v. Nevertheless, some fluids like gas and high salinity brines have a HI lower than 1 v/v and must be corrected for when interpreting the results. In addition, many hydrated minerals are encountered in sedimentary or crystalline rocks, e.g. clay minerals, gypsum, iron-hydroxides, coals, zeolites, micas and amphiboles. The NHI is commonly used to quantify the fluid volume (porosity) and as a lithological indicator (clay content, hydrogen-rich minerals), mostly in combination with the bulk density measurement.

- **Resistivity** (HRLT – High Resolution Laterolog array Tool). The HRLT measures electrical resistivities at different depths of investigation in the formation. When drilling mud filtrate invades the formation and it has a salinity that contrasts with that of the formation fluids (the chlorine ion Cl^- changes significantly the resistivity of a medium), the resistivities provide an invasion profile. Processing allows the extrapolation of the resistivity measurements far into the formation providing the true formation resistivity, as well as close to the tool providing the microresistivity or resistivity close to the borehole wall. Resistivity is used to interpret the saturation in water or hydrocarbons in pore spaces and for mineralogical identification (e.g., carbonates, clays, salt).

- **Sigma Formation Capture Cross-Section** (SIGF, from APS). In addition to the HI, the APS also measures the sigma formation capture cross-section (SIGF), that is defined as the relative ability of a material to "capture" or absorb free thermal neutrons. SIGF values vary widely with elements, and it can be used to determine the mineralogy and formation fluid contents.

- **Sonic** (MSIP – Modular Sonic Imaging Platform, also named Sonic Scanner). The MSIP measures how fast compressional and shear waves travel in the formation. A pulse sound is emitted from several tool transmitters in all directions. Tool receivers record the waves after they have travelled through a known path in the formation to the borehole wall. Waves travel at different velocities in the drilling fluid (between the tool and the borehole wall) and in the formation. Subtracting the travel time recorded by the near transmitter-receiver pairs from the

travel time recorded by far transmitter-receiver pairs provides the travel time spent in the formation only and thus discards the wave propagation in the fluid. Travel times are converted to wave slowness logs (inverse of velocity) based on the tool geometry. Compressional and shear wave slowness are used to interpret porosity, aid in mineralogy determination, for geo-mechanical and rock strength properties and they serve as calibration for seismic surveys. Other wave propagation modes are also recorded by the MSIP (oriented shear waves, Rayleigh waves, Stoneley waves). Oriented shear waves can be used to analyse the acoustic anisotropy properties of the formation. The MSIP log products require processing of the raw data to detect the different wave arrivals and transform the multiple transmitter-receiver recordings into unique slowness logs. Field processing products are basic and advanced processing products, such as the anisotropy analysis can be requested at a later stage.

- **Spectral Gamma Ray** (SGR, from the HNGS – Hostile Natural Gamma Ray Sonde). In addition to the total gamma ray, the HNGS measures the energy spectrum of the formation gamma rays. As the three main radioactive elements (potassium, thorium and uranium) are characterised by a different gamma energy, the tool can quantify those elements' content. Those concentrations can be used to quantify potassium-, uranium- or thorium-rich minerals (e.g. different clay minerals, potassic feldspars, organic matter, phosphates). The HSGR log is the sum of potassium, thorium and uranium gamma ray contributions to the total spectral gamma ray. Note that the total gamma ray from the GR and SGR tools are not necessarily quantitatively equivalent because these tools use different detectors, technologies, tool housing and calibrations. The HCGR log is the result of the HSGR log without the uranium contribution. The shading from HCGR to HSGR in log plots helps identify zones that may contain uranium-bearing organic matter and phosphates.

- **Spontaneous Potential** (SP). The SP log is a continuous measurement of the electric potential difference between an electrode in the SP tool and a surface electrode. Adjacent to shales, SP readings usually define a straight line known as the shale baseline. Next to permeable formations, the curve departs from the shale baseline; in thick permeable beds, these excursions reach a constant departure from the shale baseline, defining the "sand line". The deflection may be either to the left (negative) or to the right (positive), depending on the relative salinities of the formation water and the mud filtrate. If the formation water salinity is greater than the mud filtrate salinity (the more common case), the deflection is to the left. The movement of ions, essential to develop an SP, is possible only in rocks with some permeability, a small fraction of a millidarcy is sufficient. There is no direct relationship between the magnitude of the SP deflection and the formation's permeability or porosity.

- **Temperature** (TMP). The temperature log is acquired with the EMS tool that includes a temperature sensor. It is a measurement of the temperature in the borehole environment; thus, it is largely influenced by the temperature of mud. Since the temperature is affected by material outside the casing, a temperature log is sensitive to not only the borehole but also the formation and the casing – formation annulus. Mud temperature is generally less than that of fluids in the formation, but the temperature of the static mud is assumed to converge to the formation temperature after an infinite time. In practice, temperature logs are acquired several times after the last mud circulation, and the formation temperature is modelled based on the observed trend of temperature vs. time at each depth. On one hand, the temperature log is interpreted by looking for larger scale anomalies, or departures, from a reference gradient. This can give indications for permeable zones with fluid flow or for flow barriers hindering cross formational flow. On the other hand, localised smaller scale anomalies may correspond to the entry of borehole mud in the formation or fluid flow from the formation to the borehole. The temperature log should be interpreted together with structural geology, hydrogeology, and the other logs (e.g. images, resistivity logs).

3.2 Log data quality

3.2.1 Quality control procedures

Quality control (QC) of log data is important to guarantee their accuracy, repeatability, traceability, relevance, completeness, sufficiency, interpretability, clarity and accessibility. The generic QC procedures that were followed for each log dataset are presented as follows:

1. Digital data in .dlis format are loaded into a petrophysics software (Paradigm – Geolog) and checked for completeness (Are principal log channels, parameters and constants given?) and accessibility (Do the data load correctly when imported? Is the depth sampling rate steady and valid?).
2. Sufficient data: Do the first and last readings correspond to the interval of logs laid-out in the work programme?
3. Depth match is checked: main pass (or downlog pass if first run in hole) versus reference run, repeat pass(es) versus reference run. GR log of the EDTC tool is always used for depth correlation because it has an excellent vertical resolution and sufficient character. Schlumberger depth matches data in the field but sometimes additional depth matching is required during QC. Such depth shifts are recorded in Appendix A8 – Table of post-acquisition depth shifts.
4. Are the calipers well calibrated? This is checked by comparing caliper measurements against the nominal inner diameter of the casing.
5. Borehole shape is checked: Are there washouts? Is the borehole on gauge? Undergauge? Ovalised? Are there breakouts? Hole restrictions? If the borehole shape is not gauge, the log quality can be degraded.
6. Cable tension is checked: does the cable tension show any overpulls or stick and pull events? These events can cause a locally discontinuous depth log measurement and alter the tool positioning which impacts the log quality. The tension log is also used to check that the logger depth is consistent with the tension pick-up.
7. Graphic files (log plots) are checked for completeness, consistency and accuracy. In particular, the following sections of the graphic files are checked:
   - 7.1 Header: e.g. logging date, run number, mud parameters
   - 7.2 Borehole sketch and size / casing record: hole bit sizes and depths, casing sizes, weight and depth
   - 7.3 Borehole fluids: accuracy of mud physical parameters
   - 7.4 Remarks and equipment summary: serial numbers of equipment, completeness and accuracy of remarks
   - 7.5 Depth control parameters: right depth control procedure and log of reference
   - 7.6 Summary of run passes: top and bottom of pass, automatic bulk shift applied
   - 7.7 Log (content and display): mnemonics, description, unit, scale, colour and label of logs; display of logs, log quality control (LQC) or data copy indicator curves provided (if applicable)
   - 7.8 Channel processing parameters, tool control parameters: corrections or offsets applied to measurements, modes of acquisition, etc.
   - 7.9 Accelerometer and magnetometer crossplots provided (if applicable)
   - 7.10 Calibration reports: validity of master calibration and before calibration (if applicable), all calibrations within tolerances

8. Data repeatability for main vs. repeat passes (or downlog pass if applicable) is checked for a selection of important logs.
9. Were required, environmental corrections applied with the correct parameter values (e.g. mud salinity, mud weight, drill bit size, tool standoff, pressure / temperature).
10. Were processing parameters correctly applied (e.g. ECS minerals model options, MSIP time windows, APS lithology conversions)?
11. Data consistency is checked, including a comparison with logs from other runs via log plot and crossplots and the description of the cuttings for lithology. Are logs representative of expected lithologies and do they respond consistently?
12. Are orientation, accelerometer and magnetometer data accurate? This is essential for all data-sets that need to be oriented (e.g. borehole imagery [FMI/UBI], dipole sonic).
13. Mud resistivity and borehole temperature are checked for repeatability and checked against collected mud samples and thermometers in the logging head.
14. Quality of automatic picking on processing products (if applicable), e.g. compressional and shear wave slowness picking on semblance projections for sonic logs.

3.2.2 Bad-hole flags

To complete the data QC process, bad-hole flags were created to highlight zones where the log quality was degraded by 'bad-hole' conditions and should be viewed with caution. The methodology is presented in Tab. 3-1 and explained in detail in Appendix A7 – Badhole & unfit data flags.

Bad hole is a common issue with logging. It means that the borehole conditions are inadequate for obtaining optimum quality petrophysical logs that truly represent the formation that is being logged. The tools that either measure petrophysical properties in a space volume or must be in continuous contact with the borehole wall during logging (eccentred tools) are the most affected by bad hole. Washouts and rugose hole are the most common features that degrade the quality of the logs resulting for example in the underestimation of density and overestimation of sonic slowness.

Tab. 3-1: Bad-hole flag methodology

Bad-hole logic	**Logs used**	**Cutoff/method**
Overgauge flag	Caliper	Borehole diameter is greater than 115% of nominal drill bit size
Rugosity flag	Density correction (HDRA), acquired with TLD	The density correction log is calculated from the difference between the short- and long-spaced density measurements, an indicator of borehole rugosity and density quality. Density is not reliable when HDRA > 0.025 g/cm^3
Neutron standoff	Neutron standoff (STOF), acquired with APS	Neutron tool should be flushed with borehole wall or should have pre-determined physical standoff. If unintentional standoff, STOF > 0.35", bad hole is flagged
Density-neutron flag	Density (RHOZ) and neutron (APLC)	Systematic identification of outliers in density-neutron crossplot and comparison with analogue data from adjacent boreholes

3.3 Composite log generation

The objective of the composite log dataset is to provide a traceable quality-controlled, edited, corrected and merged dataset for all petrophysical logging data recorded across the entire length of the borehole. Petrophysical tools acquire many logs that are not directly related to petrophysical properties but are needed to control that the tool sensors worked well (e.g. mechanical or electronics status of the sensors). In addition, some logs are acquired several times in a section (e.g. GR, Temperature). Ad Terra selects a collection of the most relevant logs for formation evaluation, correlation and calibration with core or seismic data. Some 87 representative logs are thus extracted for each borehole section. These logs are:

1. quality controlled (procedures in Section 3.2.1)
2. edited e.g. to keep data points that are true responses of the borehole and formation environment
3. further corrected for the borehole environment or artefacts
4. merged into composite logs that cover the entire or most of the borehole
5. The generated composite log dataset is generated and delivered in standard digital (LAS – Log ASCII Standard) and graphic (PDF log plot) format.

A more detailed procedure for the generation of the composite log is detailed in the next subchapter. In addition, a complete report in Excel format is provided (see Appendix A) which details all relevant information about the logs and the acquisition runs. Appendix A5 – Composite log generation worksheet specifically details how the composite log dataset was generated through merging techniques.

3.3.1 Generic process

The following steps were conducted to generate the composite log dataset:

1. A bit size log was generated according to the borehole design at the time of logging (see Appendix A2 – Borehole design).
2. Logs were depth-shifted as required (see Appendix A8 – Post-acquisition depth shifts).
3. First and last readings were edited to remove values acquired before the tool sensors started reading the borehole (e.g. constant values just before/after the sensor is switched off/on) and/or before the tools started to move upward (e.g. stationary measurements close to total depth). Log readings were further edited if they did not read the borehole formation environment, e.g. logs can be impacted by the nearby casing shoe and cement, become decentralised when there are changes in the borehole diameter, or sediment infills at bottom of the borehole.
4. All logs that were not valid in cased hole were discarded. For the BOZ1-1 composite log dataset, this included all logs except for the total gamma ray log (ECGR_EDTC) from the EDTC and borehole temperature (TMP) from the EMS.
5. Bad-hole flags were created based on advanced log analysis to highlight zones where the log quality was affected by bad-hole conditions.
6. Total gamma ray log (ECGR_EDTC) was corrected for the radioactive potassium silicate in the drilling mud using the borehole potassium corrected total spectral gamma ray log (HSGR) for calibration. It was further normalised to account for attenuated readings in cased hole intervals according to standard practice. The corrected gamma ray log was then renamed GR_KCOR.
7. Poor quality sonic slowness data (DTCO, DTSM) caused by imprecise automatic picking were removed and interpolated where applicable.
8. The edited and corrected logs from each section were merged. Merging points were chosen carefully to optimise log coverage and composite log consistency. See Appendix A5 – Composite log generation.
9. Standardised log names, units and descriptions were used.
10. Logs acquired at higher resolution (e.g. RHO8, PEF8 have sample rates 0.0508 m – ⅙ ft) were resampled to the standard rate of 0.1524 m (½ ft), because the digital LAS format cannot support mixed sample rates.
11. Final log plots at a scale of 1:200 m MD, 1:1'000 m MD and 1:2'000 m MD were produced in PDF graphic file format along with digital data in LAS format.

Tab. 3-2 lists and describes all the log curves / channels that are provided in the composite log set.

Tab. 3-2: Composite log LAS channel listing

Curve / channel	**Units**	**Description**
DEPTH	M	
APLC	V/V	Near/array Corrected Limestone Porosity (Epithermal HI)
BS	IN	Bit Size
DEVI	DEG	Borehole deviation
DTCO	US/F	Delta-T Compressional
DTSM	US/F	Delta-T Shear
DWAL_MGWALK	W/W	Dry Weight Fraction Pseudo Aluminum (SpectroLith MWGALK Model)
DWAL_WALK2	W/W	Dry Weight Fraction Pseudo Aluminium (SpectroLith WALK2 Model)
DWCA_MGWALK	W/W	Dry Weight Fraction Calcium (SpectroLith MGWALK Model)
DWCA_WALK2	W/W	Dry Weight Fraction Calcium (SpectroLith WALK2 Model)
DWCL_MGWALK	W/W	Dry Weight Fraction Chlorine Associated with Salt (SpectroLith MGWALK Model)
DWCL_WALK2	W/W	Dry Weight Fraction Chlorine Associated with Salt (SpectroLith WALK2 Model)
DWFE_MGWALK	W/W	Dry Weight Fraction Iron + 0.14 Aluminum (SpectroLith MGWALK Model)
DWFE_WALK2	W/W	Dry Weight Fraction Iron + 0.14 Aluminium (SpectroLith WALK2 Model)
DWGD_MGWALK	PPM	Dry Weight Fraction Gadolinium (SpectroLith MGWALK Model)
DWGD_WALK2	PPM	Dry Weight Fraction Gadolinium (SpectroLith WALK2 Model)
DWHY_MGWALK	W/W	Dry Weight Fraction Hydrogen Associated with Coal (SpectroLith MGWALK Model)
DWHY_WALK2	W/W	Dry Weight Fraction Hydrogen Associated with Coal (SpectroLith WALK2 Model)
DWK_MGWALK	W/W	Dry Weight Fraction Potassium (SpectroLith MGWALK Model)
DWMG_MGWALK	W/W	Dry Weight Fraction Magnesium (SpectroLith MGWALK Model)
DWSI_MGWALK	W/W	Dry Weight Fraction Silicon (SpectroLith MGWALK Model)
DWSI_WALK2	W/W	Dry Weight Fraction Silicon (SpectroLith WALK2 Model)
DWSU_MGWALK	W/W	Dry Weight Fraction Sulfur (SpectroLith MGWALK Model)
DWSU_WALK2	W/W	Dry Weight Fraction Sulphur (SpectroLith WALK2 Model)
DWTI_MGWALK	W/W	Dry Weight Fraction Titanium (SpectroLith MGWALK Model)
DWTI_WALK2	W/W	Dry Weight Fraction Titanium (SpectroLith WALK2 Model)
FLAG_BADHOLE_OVERGAUGE		Overgauge Borehole Bad-Hole Flag
FLAG_BADHOLE_RUGO		Rugose Borehole Bad-Hole Flag
FLAG_BADHOLE_STOF		Neutron Porosity Standoff Bad-Hole Flag
FLAG_UNFIT_ND		Flag that indicates unfit neutron-density data for deterministic log evaluation
FPLC	V/V	Near/Far Corrected Limestone Porosity (Thermal HI)

Tab. 3-2: continued

Curve / channel	**Units**	**Description**
GR_KCOR	GAPI	Total natural radioactivity corrected for the borehole potassium (EDTC)
HAZI	DEG	Borehole azimuth
HCGR	GAPI	HNGS Computed Gamma Ray
HDAR	IN	Hole Diameter from Area
HDRA	G/C3	Density Standoff Correction
HFK	%	HNGS Formation Potassium Concentration
HSGR	GAPI	HNGS Standard Gamma-Ray
HTHO	PPM	HNGS Formation Thorium Concentration
HURA	PPM	HNGS Formation Uranium Concentration
PEF8	B/E	High Resolution Formation Photoelectric Factor
PEFZ	B/E	Standard Resolution Formation Photoelectric Factor
RD1	IN	Radius 1
RD2	IN	Radius 2
RD3	IN	Radius 3
RD4	IN	Radius 4
RD5	IN	Radius 5
RD6	IN	Radius 6
RHGE_MGWALK	G/C3	Matrix Density from Elemental Concentrations (SpectroLith MGWALK Model)
RHGE_WALK2	G/C3	Matrix Density from Elemental Concentrations (SpectroLith WALK2 Model)
RHO8	G/C3	High Resolution Formation Density
RHOZ	G/C3	Standard Resolution Formation Density
RLA0	OHMM	Apparent Resistivity from Computed Focusing Mode 0
RLA1	OHMM	Apparent Resistivity from Computed Focusing Mode 1
RLA2	OHMM	Apparent Resistivity from Computed Focusing Mode 2
RLA3	OHMM	Apparent Resistivity from Computed Focusing Mode 3
RLA4	OHMM	Apparent Resistivity from Computed Focusing Mode 4
RLA5	OHMM	Apparent Resistivity from Computed Focusing Mode 5
RT_HRLT	OHMM	HRLT True Formation Resistivity
RXO8	OHMM	Invaded Formation Resistivity filtered at 8 inches
RXOZ	OHMM	Invaded Formation Resistivity filtered at 18 inches
RXO_HRLT	OHMM	HRLT Invaded Zone Resistivity
SIGF	CU	Formation Capture Cross-Section
SP	MV	Spontaneous Potential
STOF	IN	Effective Standoff in Limestone
SV	MPa	Overburden vertical stress (Sv)
TMP	DEGC	Mud Temperature
U8	B/C3	High Resolution Volumetric Photoelectric Factor

Tab. 3-2: continued

Curve / channel	**Units**	**Description**
UZ	B/C3	Volumetric Photoelectric Factor
WANH_MGWALK *	W/W	Dry Weight Fraction Anhydrite/Gypsum (SpectroLith MGWALK Model)
WANH_WALK2 *	W/W	Dry Weight Fraction Anhydrite / Gypsum (SpectroLith WALK2 Model)
WCAR_MGWALK *	W/W	Dry Weight Fraction Carbonate (SpectroLith MGWALK Model)
WCAR_WALK2 *	W/W	Dry Weight Fraction Carbonate (SpectroLith WALK2 Model)
WCLA_MGWALK *	W/W	Dry Weight Fraction Clay (SpectroLith MGWALK Model)
WCLA_WALK2 *	W/W	Dry Weight Fraction Clay (SpectroLith WALK2 Model)
WCLC_MGWALK *	W/W	Dry Weight Fraction Calcite (SpectroLith MGWALK Model)
WCOA_MGWALK *	W/W	Dry Weight Fraction Coal (SpectroLith MGWALK Model)
WCOA_WALK2 *	W/W	Dry Weight Fraction Coal (SpectroLith WALK2 Model)
WDOL_MGWALK *	W/W	Dry Weight Fraction Dolomite (SpectroLith MGWALK Model)
WEVA_WALK2 *	W/W	Dry Weight Fraction Salt (SpectroLith WALK2 Model)
WPYR_MGWALK *	W/W	Dry Weight Fraction Pyrite (SpectroLith MGWALK Model)
WPYR_WALK2 *	W/W	Dry Weight Fraction Pyrite (SpectroLith WALK2 Model)
WQFM_MGWALK *	W/W	Dry Weight Fraction Quartz+Feldspar+Mica (QFM) (SpectroLith MGWALK Model)
WQFM_WALK2 *	W/W	Dry Weight Fraction Quartz+Feldspar+Mica (QFM) (SpectroLith WALK2 Model)
WSID_MGWALK *	W/W	Dry Weight Fraction Siderite (SpectroLith MGWALK Model)
WSID_WALK2 *	W/W	Dry Weight Fraction Siderite (SpectroLith WALK2 Model)

* Qualitative data should only be used as a lithology indicator.

3.3.2 Gaps in log coverage

Optimising the petrophysical log and MHF testing coverage was an objective of the logging and testing campaigns, in particular for the potential Opalinus Clay rock host. Despite best efforts, gaps in log coverage are an inherent limitation in wireline logging operations.

Complete log coverage at changes in drilling section is possible if the acquisition of the lowermost part of the drilling section is repeated later with the acquisition of the uppermost part of the drilling section below. Logs acquired with the same sensor, which overlap over two sections can then be merged providing complete coverage. This is not always possible due to limitations related to tool string geometry, borehole conditions and borehole design. Examples include:

- Cuttings infill the bottom of the hole preventing the tool string from reaching total depth.
- The tool string should not tag the bottom hole with certain fragile tools (e.g. UBI).
- The offset of the sensors relative to the bottom of the tool string.
- The rathole clearance (space between casing shoe and the bottom of the drilled hole) available for logging in the section below is too short. If the casing shoe is too close to the bottom of the section and the lowermost part of the open hole was not logged before casing installation, some log coverage will be lost.
- The rathole available for logging in the section below is first enlarged, and its diameter is different (e.g. 12¼") from that of the cored section below (6⅜"). Abrupt changes in borehole size are not favorable for logging because they are often associated with bad hole and eccentered tools in contact with the borehole wall acquire logs of degraded quality, causing gaps in log coverage.

The above factors were taken into consideration in the design of work programmes. For each logging campaign, project guidelines defined the balance between the optimisation of log coverage (short tool strings, more runs, longer campaign) and saving rig time and associated costs (slightly longer tool strings, less runs, shorter campaign).

For the main drilling sections where petrophysical logs were acquired (Section II to TD), a summary of the meterage of logged data and the percentage of total depth this data represents, is summarised in Tab. 3-3. The Opalinus Clay and bounding formations (Dogger – Lias) were examined in greater detail. Complete log coverage was acquired in these formations.

Tab. 3-3: Summary of Petrophysical Log Coverage from Drilling Section II to TD

Measurement	**Section II to TD** (470.0 m to 1'288.12 m MD)		**Opalinus Clay and Bounding Formations (Dogger to Lias)** (696.03 m to 922.71 m MD)	
	Meterage [m]	**Coverage** [%]	**Meterage** [m]	**Coverage** [%]
Caliper	815.03	99.6	226.68	100.0
Borehole orientation	813.70	99.5	226.68	100.0
Total Gamma Ray	812.45	99.3	226.68	100.0
Spontaneous Potential	811.71	99.2	226.68	100.0
Spectral Gamma Ray	811.42	99.2	226.68	100.0
Density	807.37	98.7	226.68	100.0
Photoelectric Factor	807.37	98.7	226.68	100.0
Microresistivity	805.69	98.5	226.68	100.0
Neutron (NHI)	804.22	98.3	226.68	100.0
Sigma Formation Capture Cross-Section	804.22	98.3	226.68	100.0
Resistivity	787.19	96.2	226.68	100.0
Sonic	808.79	98.9	226.68	100.0
Element Spectroscopy	813.36	99.4	226.68	100.0
Ultrasonic Borehole Imagery	578.29	70.7	226.68	100.0
Microresistivity Borehole Imagery	814.33	99.5	226.68	100.0

The depths at which there were gaps in log coverage in the final composite dataset are detailed in Appendix A5 – Composite log generation.

3.4 Petrophysical logging results and description

The main features of the petrophysical logs of the composite dataset are described below by litho-stratigraphic units.

3.4.1 Tertiary: OSM, OMM, and Siderolithikum (0 to 98 m MD)

Only the total GR was acquired in cased hole of Section I of the borehole. The log quality was influenced by the large drill bit size (23") and the attenuated GR emitted by the formation through the cemented casing. The total GR log could therefore not be corrected, and it was discarded.

3.4.2 Malm: Villigen Formation and Wildegg Formation (98 to 406.72 m MD)

No valid logs were acquired above the 7⅝" auxiliary casing set at 253.2 m MD in the Wildegg Formation, in Section II of the borehole.

Log responses reflect the borehole lithology well except in the 8½" rat-hole immediately below the 7⅝" auxiliary casing, where the borehole wall rugosity deteriorated the response of the TLD and APS tool logs (density, photoelectric factor, microresistivity and neutron).

Logs in the Wildegg Formation are characterised by (Fig. 3-1):

- Low to moderate clay content: low to moderate total GR (GR_KCOR: 6 to 71 GAPI; mean = 38 GAPI), spectral GR (e.g. thorium HTHO: 0.7 to 10.4 ppm; mean = 5.1 ppm) and sigma (SIGF: 9.8 to 31.0 CU; mean = 19.8 CU).
- Calcite is the dominant mineral: narrow density-neutron separation when displayed in a lime-stone-compatible scale (density [RHOZ] and neutron [APLC] readings in low clay limestone (300 m to 318 m MD) are 2.71 g/cm^3 and 0.0 v/v, respectively), the calcium dry weight fraction (DWCA) and photoelectric factor (PEFZ) are reading values close to that of pure calcite (0.394 W/W and 5.1 B/E, respectively).
- In the low clay limestone (GR_KCOR < 15 GAPI), porosity is low, density is high (rarely lower than 2.62 g/cm^3; mean: 2.65 g/cm^3) and sonic (DTCO) rarely exceeds 70 µs/ft.

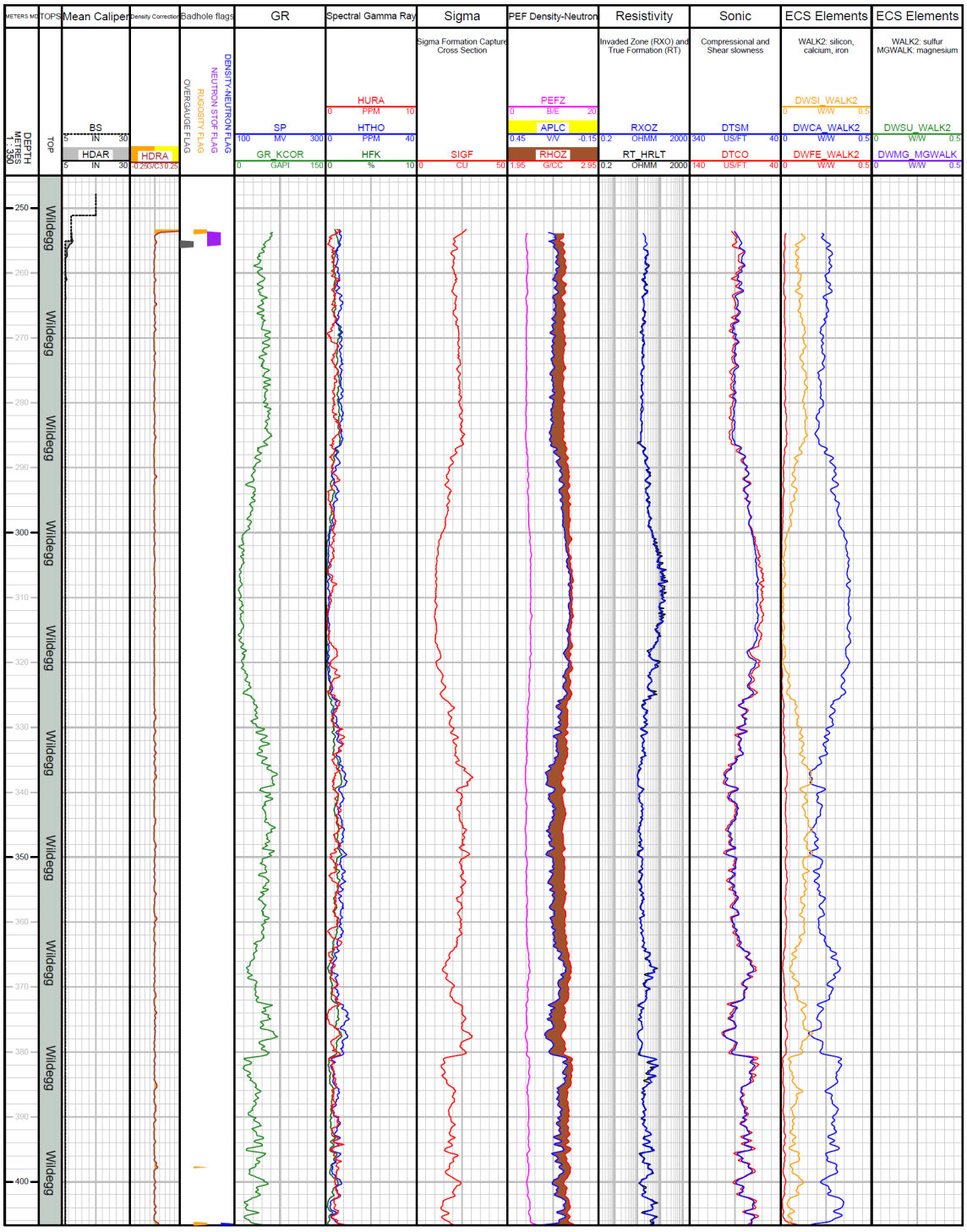

Fig. 3-1: Main logs of the composite dataset in the Wildegg Formation

3.4.3 Ifenthal Formation to Passwang Formation (406.72 to 530.32 m MD)

The top of the Dogger (Ifenthal Formation) can be identified by an increase in total GR, a wide separation in the density-neutron logs (displayed in a limestone-compatible scale) and an increase in iron concentration (DWFE), all indicative of siderite, iron oxide or hydroxide bearing rocks (Fig. 3-2).

Due to good-hole conditions, log responses reflect the borehole lithology well from the Ifenthal Formation to the Passwang Formation. Logs have the following attributes:

- Moderately low (Hauptrogenstein Formation) to moderate high (Passwang Formation) clay content as shown by the total GR (18 to 109 GAPI), SIGF (12.7 to 37.5 CU) and HTHO (2.4 to 24.7 ppm).

- The occurrence of siderite, iron oxide or hydroxide is typical in these formations: a wide separation in the density-neutron, high total and spectral GR (especially thorium HTHO up to 24.7 ppm and uranium HURA up to 4.4 ppm), high iron concentration (DWFE: above 0.05 W/W) and high photoelectric factor (PEFZ up to 7.6 B/E).

- The matrix mineralogy is dominated by calcite: in the lowest clay and low iron zones PEFZ is in the range of 3.5 to 5.9 B/E, while calcium is relatively high (DWCA: up to 0.32 W/W; 0.394 W/W in pure calcite), which is typical of marls. In the lowermost Passwang Formation, the separation between the density-neutron is low while silicon is relatively high (DWFE: up to 0.27 W/W; 0.467 W/W in pure quartz), indicating a siliciclastic component in the matrix mineralogy.
- The spectral GR potassium (HFK) and thorium (HTHO) logs suggest the presence of both non-potassic (e.g., kaolinite, smectite) and potassic (e.g., illite) clay minerals in the clay-rich zones.

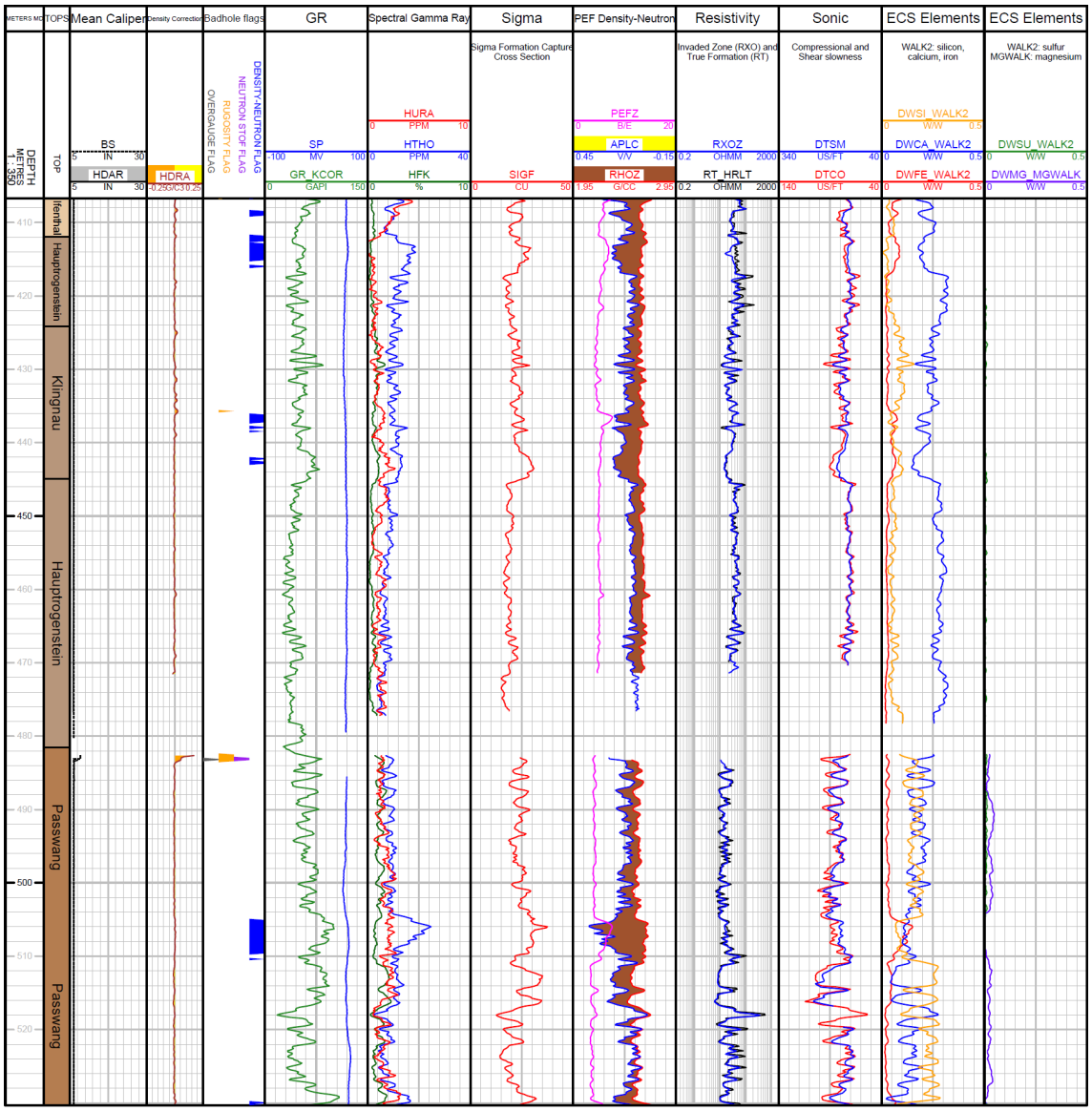

Fig. 3-2: Main logs of the composite dataset in the Ifenthal Formation to Passwang Formation

3.4.4 Opalinus Clay (530.32 to 651.46 m MD)

Contrary to all adjacent TBO boreholes except BOZ2-1, the top Opalinus Clay is characterised by a decrease in clay content indicators (e.g. total GR [GR_KCOR], sigma (SIGF) and thorium [HTHO]), because the base of the Passwang Formation has a higher clay content than the uppermost Opalinus Clay.

Log responses reflect the borehole lithology well because hole conditions were excellent for wireline logging. In the Opalinus Clay, logs have the following attributes (Fig. 3-3):

- Consistently moderate to high clay content: GR_KCOR ranges from 54 to 113 GAPI; SIGF correlates very well (positively) to GR_KCOR, ranging from 21.4 to 47.9 CU; the compressional wave slowness DTCO was high (slow formation) and generally above 87 µs/ft; the density-neutron separation is typical of lithologies with high clay content.
- The upper part of the formation has a higher carbonate content (DWCA) than adjacent boreholes, which decreases gradually downwards. A few carbonate streaks are also present in the upper part of the formation at 548.9, 552.5 and 576.2 m MD as shown by the combined increase in density and decrease in neutron, with values approaching those of pure calcite (RHOZ: 2.71 g/cm^3; APLC: 0.0 v/v), an increase in calcium (DWCA up to 0.10 W/W) and an increase in the resistivity logs (e.g. RT_HRLT).
- While the clay content is relatively homogeneous throughout, two distinct trends can be observed. In the upper part of the formation above 587.0 m MD, the clay content is lower and the carbonate content is higher and more variable than in the lower Opalinus Clay. Below 587.0 m MD, the clay content gradually increases with depth as shown by the gradual widening of the density-neutron separation and increase in sigma. Carbonate streaks are absent in the lower part of the formation.
- The spectral GR potassium (HFK) and thorium (HTHO) logs suggest the presence of both non-potassic (e.g., kaolinite, smectite) and potassic (e.g., illite) clay minerals in the clay-rich zones.
- Matrix mineralogy is complex. Both calcium (DWCA) and silicon (DWSI) concentrations are often higher than those in smectite clays (DWCA: 0.00 to 0.15 W/W; DWSI: 0.16 to 0.28 W/W; excluding the carbonate streaks), which suggests siliciclastic and carbonate components in the matrix.

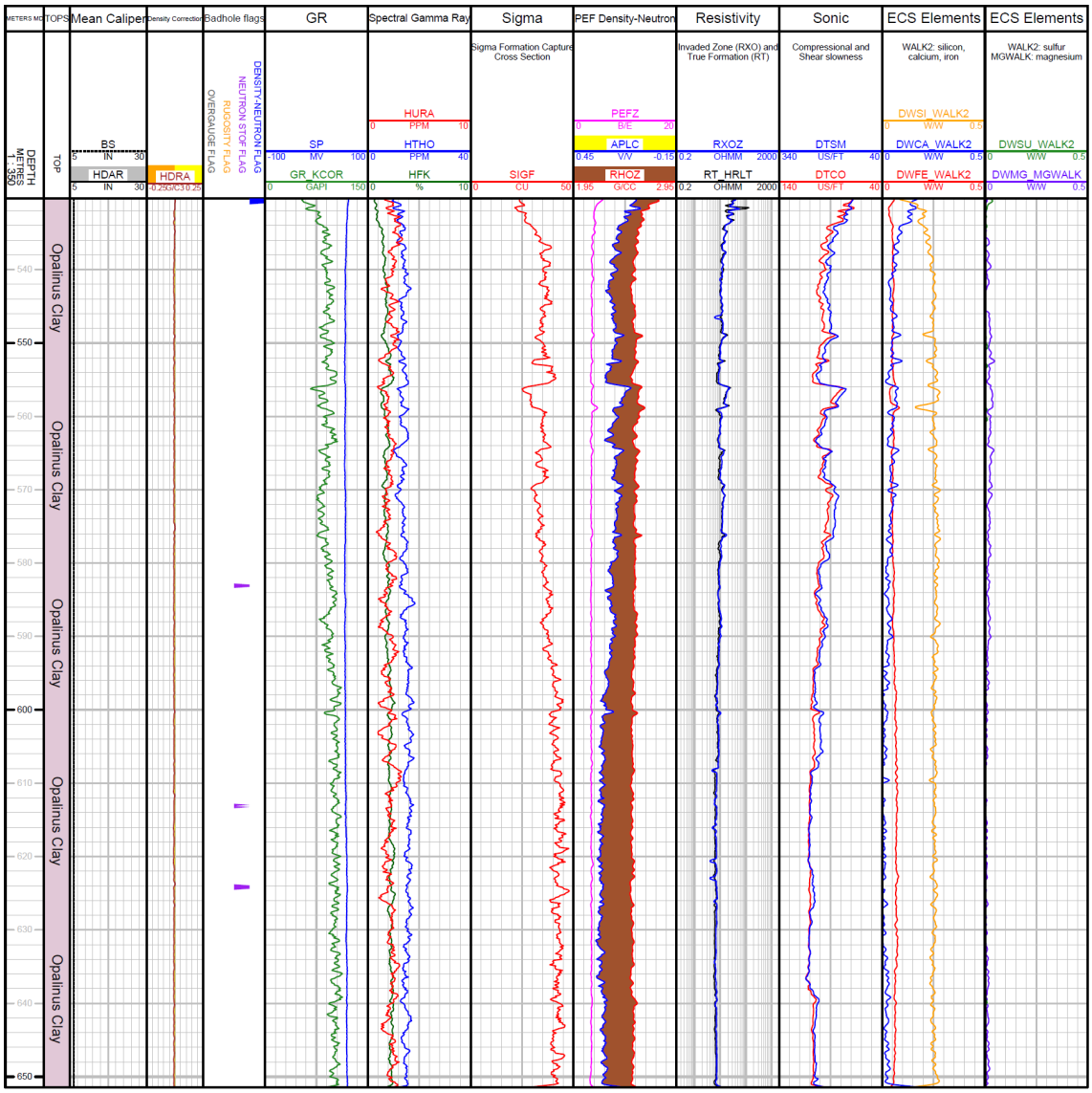

Fig. 3-3: Main logs of the composite dataset in the Opalinus Clay

3.4.5 Staffelegg Formation (651.46 to 688.76 m MD)

The top of the Lias (Staffelegg Formation) can be identified by a decrease in total GR (GR_KCOR) and sigma (SIGF), a narrower separation in the density-neutron logs in a limestone-compatible scale and an increase in calcium contents (DWCA) (Fig. 3-4).

Hole conditions were good in the Staffelegg Formation. Logs respond well to the borehole lithology having the following attributes:

- Highly variable clay content: total GR (42 to 191 GAPI), sigma (13.8 to 51.5 CU) and thorium (3.1 to 17.0 ppm), e.g. low clay content in the Beggingen Member (675.75 to 679.15 m MD) but intermediate to high clay content in the Schambelen Member (679.15 to 688.76 m MD).
- Organic matter is likely present: the high total GR zones (GR_KCOR > 120 GAPI) correspond with the uranium peaks (HURA: up to 15.7 ppm).
- Pyrite is an important accessory mineral in several members of the Staffelegg Formation (Gross Wolf, Grünschholz/Breitenmatt/Rickenbach, Grünschholz and Schambelen Members): Sulphur concentration (DWSU) ranges from 0 to 0.03 W/W; the photoelectric factor (PEFZ), a reactive marker of pyrite, reaches high values of 6.5 B/E.
- Matrix mineralogy is dominated by carbonate: calcium (DWCA) varies between 0 and 0.31 W/W (pure calcite: 0.394 W/W); however, mineralogy remains complex, the multi-mineral interpretation detailed in Dossier X will help to better understand this complex mineralogy.

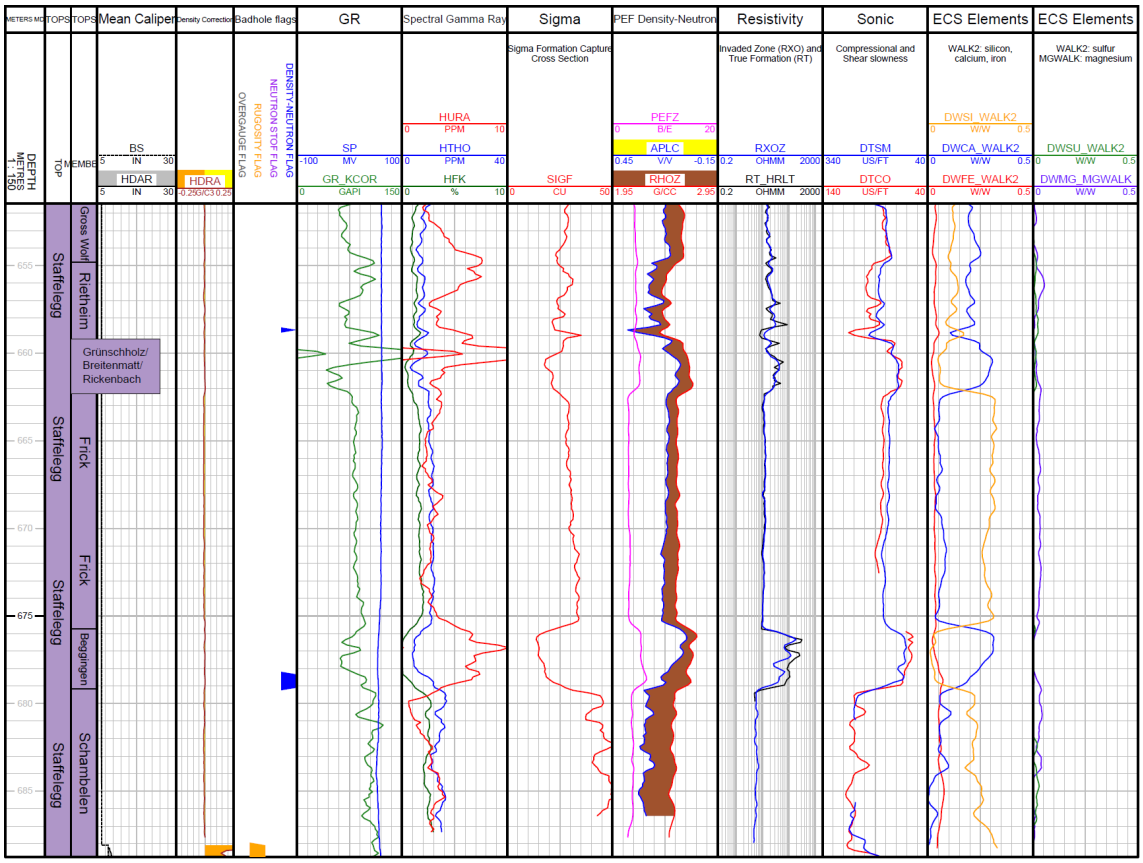

Fig. 3-4: Main logs of the composite dataset in the Staffelegg Formation

3.4.6 Klettgau Formation (688.76 to 720.21 m MD)

The bottom of the Lias (Staffelegg Formation) could not be logged in open hole because the rathole clearance below Section III was insufficient. The top of the Triassic (Klettgau Formation) was logged in an enlarged open hole (rathole). Thus, the change in log attributes between the two formations could not be discerned.

Hole conditions were good in the Klettgau Formation except in its uppermost part due to the rathole. Logs respond well to the borehole lithology having the following attributes (Fig. 3-5):

- Highly variable clay content: total GR ranges from 19 to 267 GAPI, sigma from 9.9 to 40.8 CU and thorium from 1.4 to 16.9 ppm; clay indicators have a bimodal distribution that reflects zones with a low clay content (702.80 to 709.02 m MD, Gansingen Member), and zones with intermediate to high clay contents (688.76 to 702.80 m MD, Gruhalde Member; 709.02 to 720.21 m MD, Ergolz Member).
- Organic matter is likely present at the base of the Ergolz Member: the highest total GR readings (GR_KCOR > 140 GAPI) correspond to high uranium peaks (HURA: up to 14.2 ppm).
- Carbonate is the main matrix component in the upper Klettgau Formation down to 708.7 m MD in the Gansingen Member, indicated by the intermediate to high calcium concentration (DWCA: 0.09 to 0.35 W/W; pure calcite: 0.394 W/W). The carbonate has a dolomitic signature, as shown by the magnesium concentration (DWMG: 0.05 to 0.11 W/W) and the photoelectric factor (PEFZ) whose mean value (3.4 B/E) is close to that of pure dolomite (3.1 B/E).
- From 708.7 m MD to the base of the Ergolz Member, the calcium concentration is low (mean DWCA: 0.03 W/W) and the silicon concentration increases up to 0.35 W/W. Despite the intermediate to high clay content, the density-neutron separation in the limestone-compatible scale is limited, which suggests a siliciclastic matrix (density would be to the left of neutron in the limestone-compatible scale in pure quartz lithology).

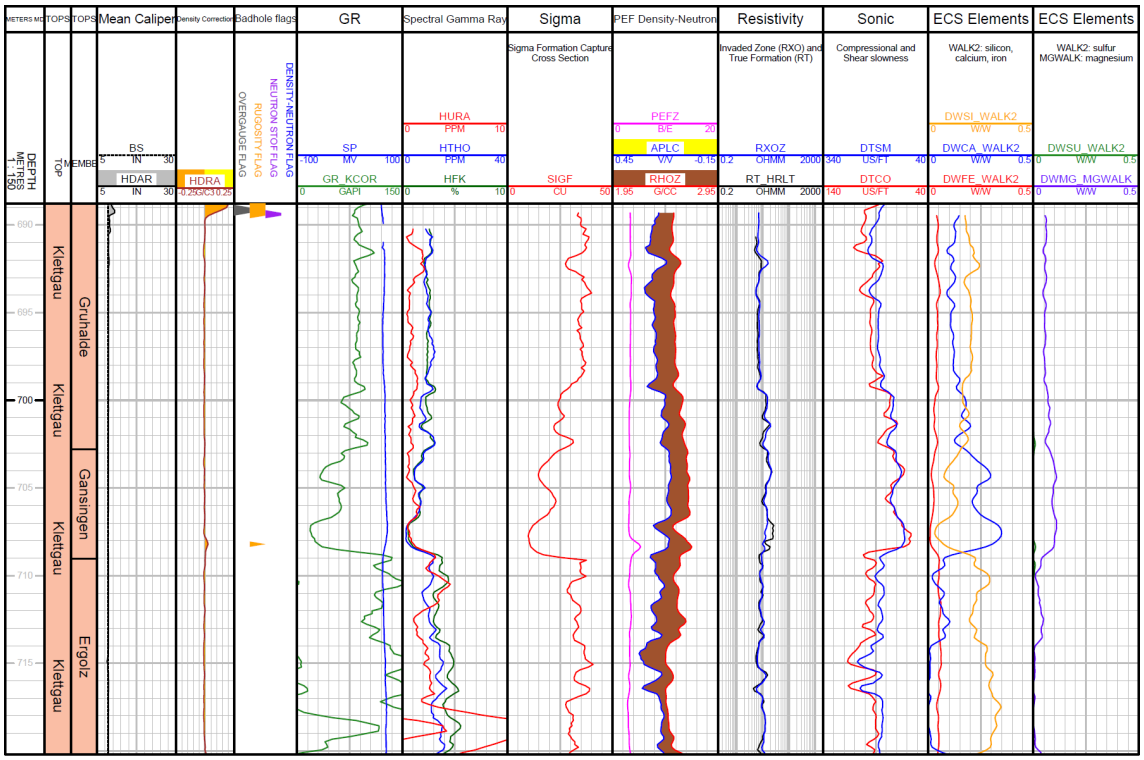

Fig. 3-5: Main logs of the composite dataset in the Klettgau Formation

3.4.7 Bänkerjoch Formation (720.21 to 812.45 m MD)

The top of the Bänkerjoch Formation is characterised by a shift to lower values of total GR (GR_KCOR), thorium (HTHO) and sigma (SIGF). At the same time, sulphur (DWSU) and calcium (DWCA) concentrations increase. These log characteristics show the onset of the significant concentrations of anhydrite in this formation.

Hole conditions were mostly good in the Bänkerjoch Formation and logs responded well to borehole lithology. Logs show the following attributes (Fig. 3-6):

- Rapid variations in most logs at the metre scale or less, which suggests two main alternating lithologies. One having high sulphur (DWSU: up to 0.22 W/W) and calcium concentrations (DWCA: up to 0.34 W/W), high photoelectric factor (mean PEFZ: 4.1 B/E) and low to intermediate total GR which suggest predominantly anhydrite bearing beds. The alternate beds have higher clay contents as indicated by the lower sulphur and calcium concentrations, high silicon (DWSI: up to 0.24 W/W) and intermediate to high total GR.
- The density-neutron separation in the limestone-compatible scale remains similar for both lithologies but logs shift from left to right for the clay and anhydrite dominant endmembers, respectively.
- Due to the limited vertical resolution of the logging tool, often higher than 10" (e.g. APS: 14"), the alternating lithologies are not necessarily correctly reflected in the logs. The logging tools average the physical and chemical properties over a fixed volume, which means that centimetre scale beds are represented as a mixture of anhydrite and clays for a given depth.

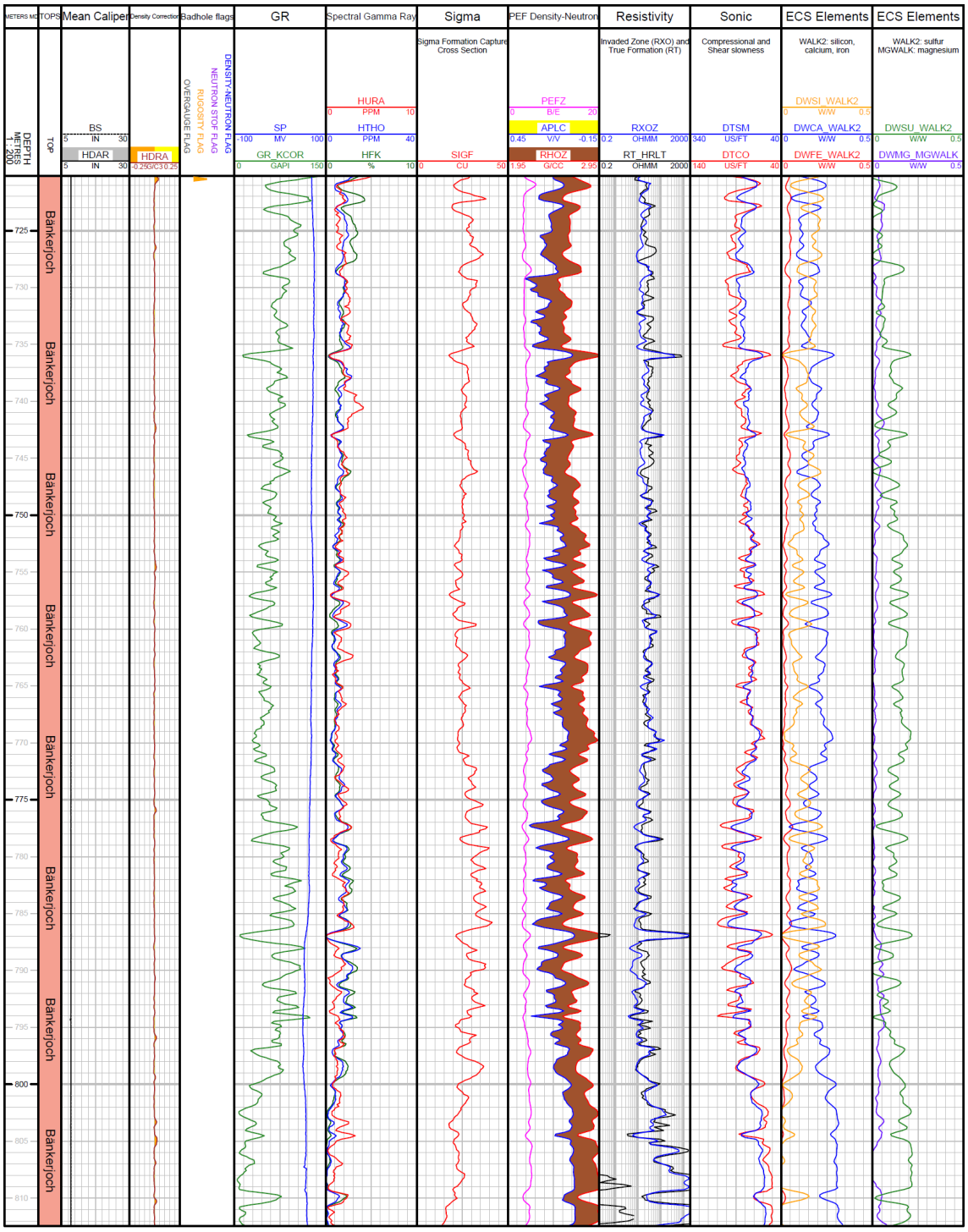

Fig. 3-6: Main logs of the composite dataset in the Bänkerjoch Formation

3.4.8 Schinznach Formation (812.45 to 876.05 m MD)

The top of the Schinznach Formation is identified by the disappearance of the sulphur content (DWSU) and a decrease in the photoelectric factor (PEFZ) and sigma (SIGF) below the lowest anhydrite bed of the Bänkerjoch Formation.

Hole conditions were mostly good in the Schinznach Formation and logs responded well to the borehole lithology. Logs are characterised by the following attributes (Fig. 3-7):

- Low to moderately low clay contents as shown by the total GR (GR_KCOR: 9 to 51 GAPI), sigma (SIGF: 7.8 and 13.9 CU) and thorium (HTHO: 0.3 to 3.8 ppm), except in the interval from 814.7 to 816.9 m MD in the Asp Member where a clay-rich layer is present.
- Carbonate is the main matrix mineral as shown by the fast sonic (DTCO, DTSM), low silicon (DWSI) and high calcium concentrations (DWCA: up to 0.40 W/W; pure calcite is 0.394 W/W for comparison).
- From the top of the Schinznach Formation to 848.6 m MD, the carbonate has a mostly dolomitic signature as shown by the photoelectric factor (PEFZ) whose mean value is that of pure dolomite (3.1 B/E) and the high magnesium concentration (DWMG: up to 0.13 W/W), whilst the density-neutron separation is positive, and the clay content is low. The large separation between the shallow (RXOZ) and deep (RT_HRLT) resistivities indicate invasion of mud filtrate into the permeable formation across several zones.
- From 848.6 m MD to the bottom of the Schinznach Formation, the mean photoelectric value (4.6 B/E) is close to that of pure calcite (5.1 B/E) and the density-neutron separation is slightly positive or absent suggesting that the carbonates are mostly limestones and dolomitic limestones.

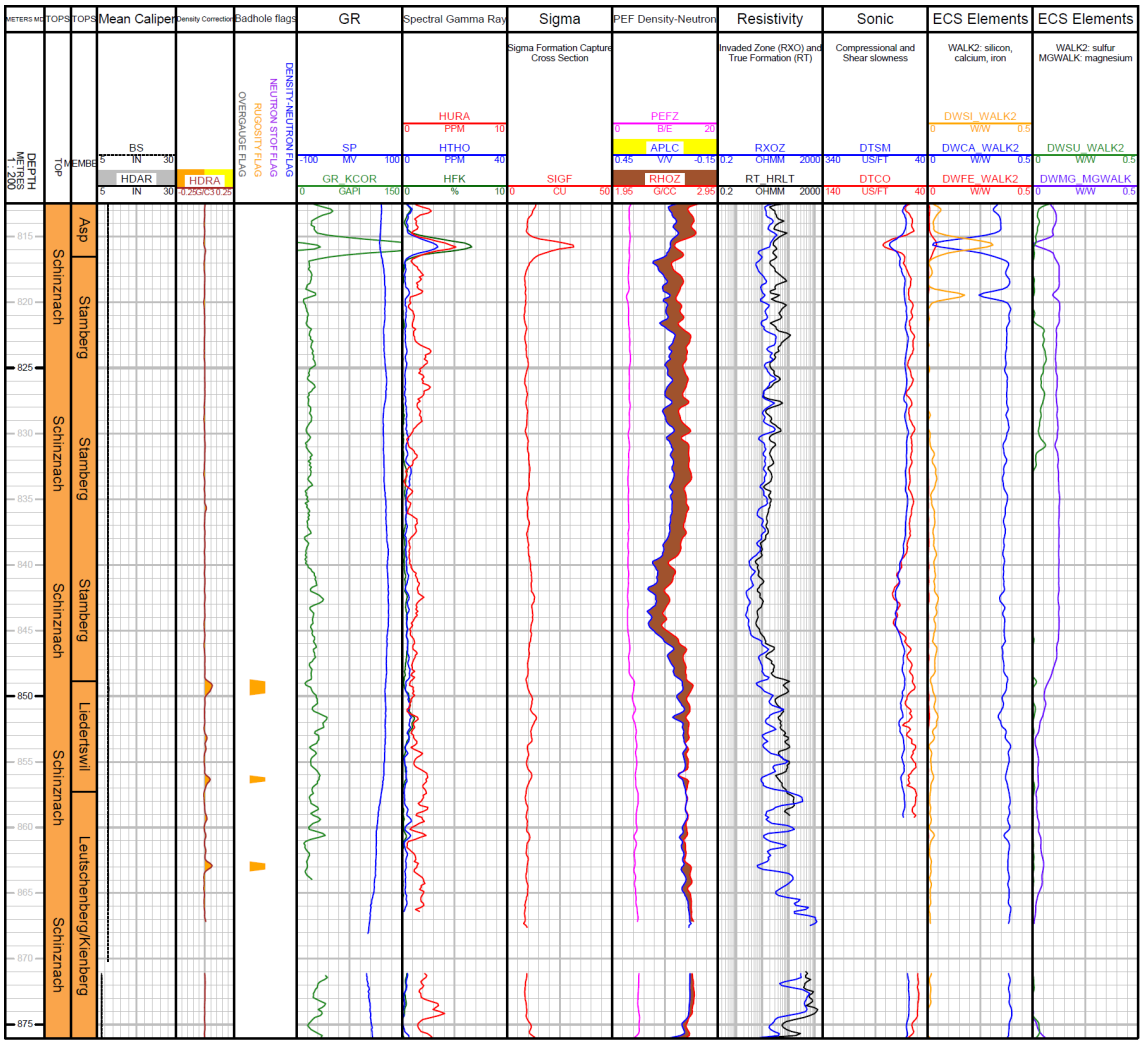

Fig. 3-7: Main logs of the composite dataset in the Schinznach Formation

3.4.9 Zeglingen Formation (876.05 to 922.30 m MD)

The top of the Zeglingen Formation corresponds to a sharp transition from a clay-free, calcite-dominated carbonate to a low clay dolostone as indicated by the decrease in calcium content (DWCA), increase in silicon content (DWSI) and a reduction in the photoelectric factor (PEFZ).

Hole conditions were good except in the short «Salzlager» (from 914.22 to 915.54 m MD), where there were washouts and rugosity. Outside this zone, logs responded well to borehole lithology. The Zeglingen Formation is characterised by the following (Fig. 3-8):

- Low to moderately high clay content: total GR (GR_KCOR: 4 to 123 GAPI), sigma (SIGF: 9.3 to 56.1 CU) and thorium (HTHO: 0.3 to 11.3 ppm).
- Density (RHOZ) is often greater than 2.9 g/cm^3 suggesting the presence of anhydrite. This is supported by the photoelectric factor (PEFZ) that is close to the value of pure anhydrite (5.05 B/E) and the significant sulphur content (DWSU: up to 0.23 W/W; value in anhydrite: 0.236 W/W).
- From the top of the Zeglingen Formation to 898.4 m MD, logs indicate less anhydrite, and dolomite is the main mineral component: the photoelectric factor values are close to that of pure dolomite (3.1 B/E), and the magnesium content (DWCA) ranges from 0 to 0.13 W/W.
- The «Salzlager» is characterised by very low densities (RHOZ: lower than 2.45 g/cm^3) and very high sigma (SIGF: up to 56 CU), which are typical for salt deposits.

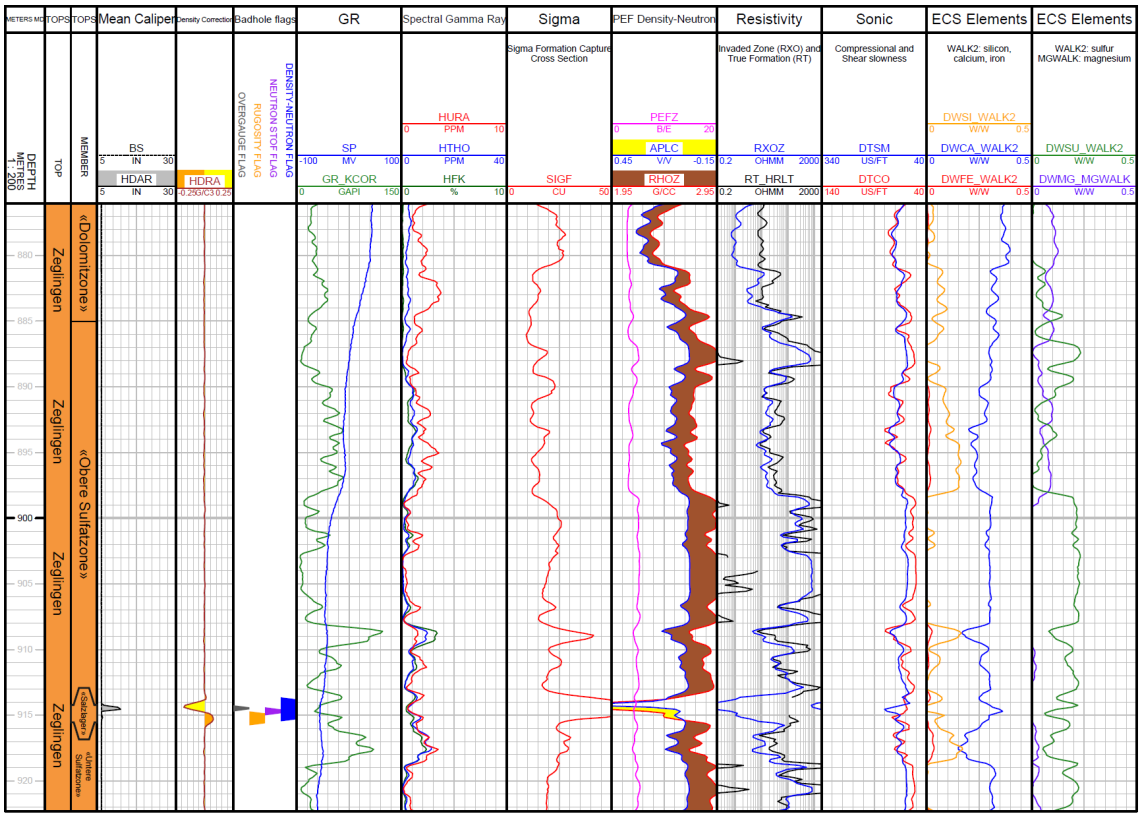

Fig. 3-8: Main logs of the composite dataset in the Zeglingen Formation

3.4.10 Kaiseraugst Formation (922.30 to 967.70 m MD)

The top of the Kaisergaust Formation is defined as the base of the last massive anhydrite bed of the overlying Zeglingen Formation. It is thus characterised by a decrease in the sulphur content (DWSU). In addition, the clay content markers slightly increase: total GR (GR_KCOR), silicon content (DWSI) and thorium (HTHO).

Due to the good-hole conditions, log responses reflect the borehole lithology well (Fig. 3-9). Logs in the Kaiseraugst Formation have the following attributes:

- Intermediate to high clay content as shown by the total GR (GR_KCOR: 8 to 177 GAPI), sigma (SIGF: 15.9 to 40.9 CU) and thorium (HTHO: 3.4 to 16.6 ppm), except in a short interval from 998.6 to 1'000.8 m MD that is rich in anhydrite. The «Wellenmergel» has the highest clay content. The unusually high values shown by the clay indicators in the argillaceous marlstones described by wellsite geologists are likely due to the presence of bituminous shales (described in Jordan 2016). Gas while drilling supports this theory as total gas measurements showed a slight increase (< 1%). Core measurements will allow a better understanding of the rock components.
- The anhydrite layer in the lower «Obricularismergel» (from 927.9 to 930.0 m MD) is characterised by its high sulphur content (DWSU: up to 0.22 W/W; pure anhydrite: 0.236 W/W), low total GR (GR_KCOR: mean = 25 GAPI) and high resistivities (e.g. RT_HRLT).
- Below the anhydrite layer (930 m MD) to the base of the «Wellenmergel» (957.25 m MD), logs show relatively homogeneous values, e.g. an intermediate density-neutron separation in the limestone-compatible scale, intermediate sonic (DTCO: 72 to 104 µs/ft) and consistent iron concentrations (DWFE: 0.03 to 0.06 W/W). These suggest moderately high to high clay contents as is common in argillaceous marlstones. Magnesium content ranges up to 0.06 W/W, which suggests a dolomitic component in the matrix mineralogy.
- Matrix mineralogy indicators such as silicon (DWSI), calcium (DWCA) and the photoelectric factor (PEFZ) are variable and not consistent with clay indicators suggesting that the matrix mineralogy in the Kaiseraugst Formation is composed of both carbonates and siliciclastics.
- Clay minerals could not be identified based on the qualitative spectral GR potassium (HFK) vs. thorium (HTHO) crossplot because spectral GR logs were biased by the bituminous shales.

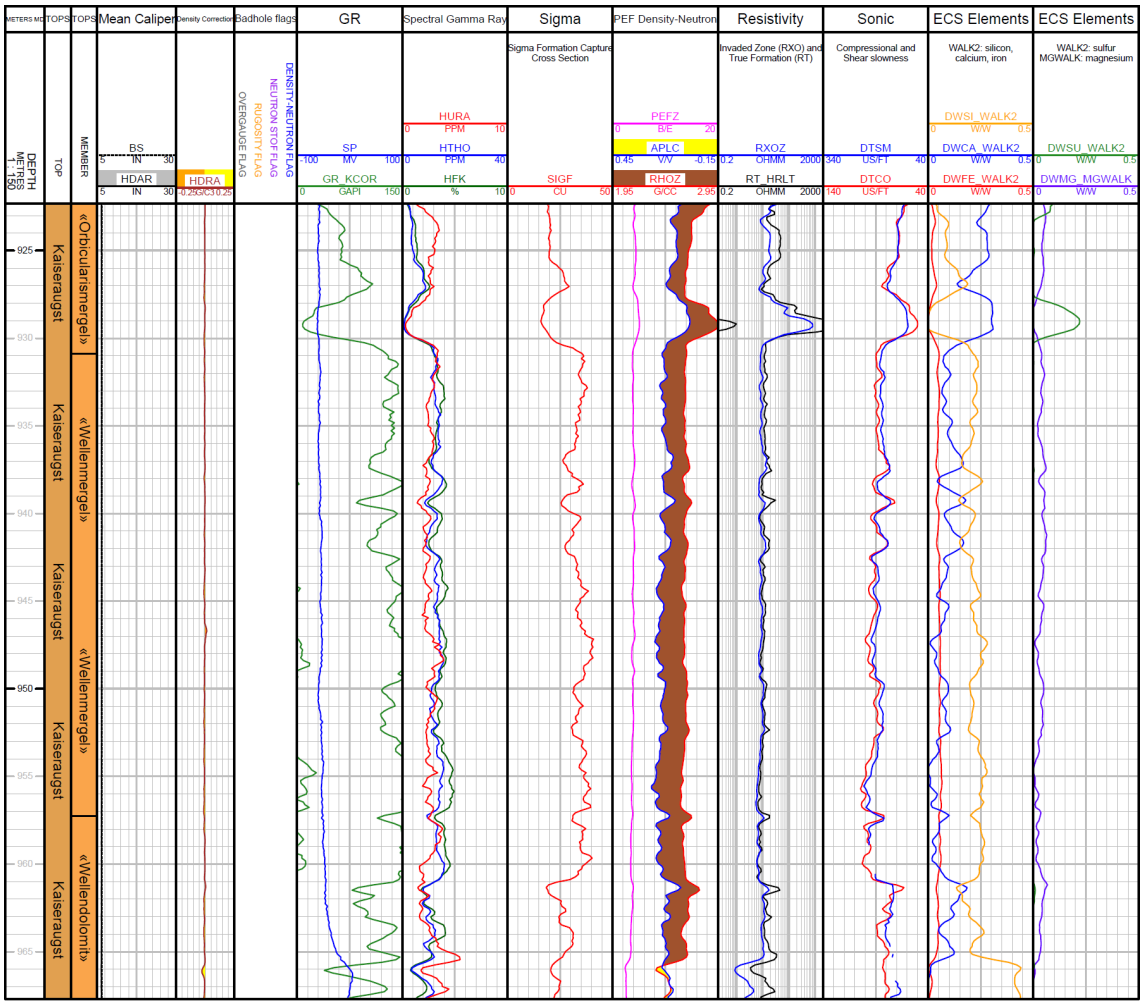

Fig. 3-9: Main logs of the composite dataset in the Kaiseraugst Formation

3.4.11 Dinkelberg Formation (967.70 to 989.83 m MD)

The top of the Dinkelberg Formation corresponds to the bottom of a gradual transition from the heterogeneous carbonates, claystones and sandstones of the Kaiseraugst Formation to low-clay sandstones from 965.3 m to 967.7 m MD, which is represented in the logs by an increase in the silicon content (DWSI) and a decrease in calcium (DWCA), as well with a very distinctive change in the density-neutron separation, where the density log shifts to the left of the neutron log ("cross-over" in a limestone-compatible scale, shaded yellow).

Logs respond well to lithology in this formation because hole conditions were good and are characterised by the following attributes (Fig. 3-10):

- Logs often show a high corrected total GR (GR_KCOR) ranging from 27 to 238 GAPI, despite the crossover in the density-neutron separation that is indicative of a low clay content and mineralogy dominated by siliciclastics. This is typical for siltstones and sandstones that contain slightly radioactive minerals such as K-feldspar and mica (and are better quantified by the stochastic, multimineral analysis described in Dossier X). The relatively high potassium concentrations (HFK), ranging from 0.4 to 3.2%, also suggest the presence of radioactive minerals.
- Photoelectric factor values (PEFZ) are close to that of pure quartz (1.8 B/E) in the Dinkelberg Formation, averaging at 2.5 B/E. The silicon content (DWSI) also suggests the presence of significant quartz, ranging from 0.40 to 0.47 W/W (pure quartz: 0.467 W/W).
- The large separation between the shallow (RXOZ) and deep (RT_HRLT) resistivities indicates a permeable formation that has been invaded by the mud filtrate.

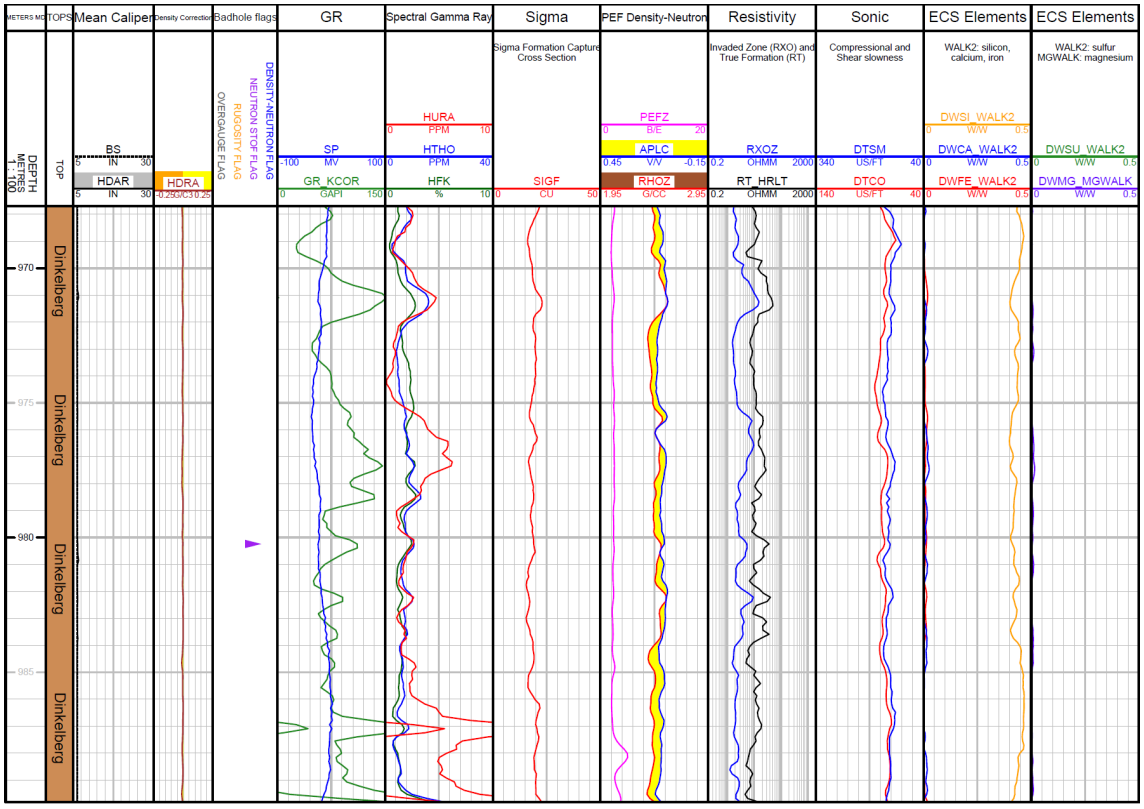

Fig. 3-10: Main logs of the composite dataset in the Dinkelberg Formation

3.4.12 Weitenau Formation (989.83 to 1'037.31 m MD)

The top of the Weitenau Formation is characterised by sharp increases in the clay indicators such as total GR (GR_KCOR) and sigma (SIGF).

Logs respond well to lithology in this formation because hole conditions were good (Fig. 3-11). Logs in the Weitenau Formation have the following attributes:

- Very high total GR, ranging from 211 to 382 GAPI, with a low density-neutron separation in the limestone-compatible scale, indicate relatively low clay contents. This is typical for siltstones and sandstones that contain radioactive minerals such as K-feldspar and mica.
- In a few zones, "crossover" is observed in the density-neutron separation (shaded yellow) indicating the presence of siliciclastic minerals such as quartz (and feldspars). This observation is supported by the high silicon content (DWSI: 0.32 to 0.43 W/W) and the low photoelectric factor (mean PEFZ: 3.5 B/E).
- Mineralogy is likely heterogeneous, which is best shown by the variations in spectral GR contributions (potassium: HFK; thorium: HTHO; uranium: HURA).

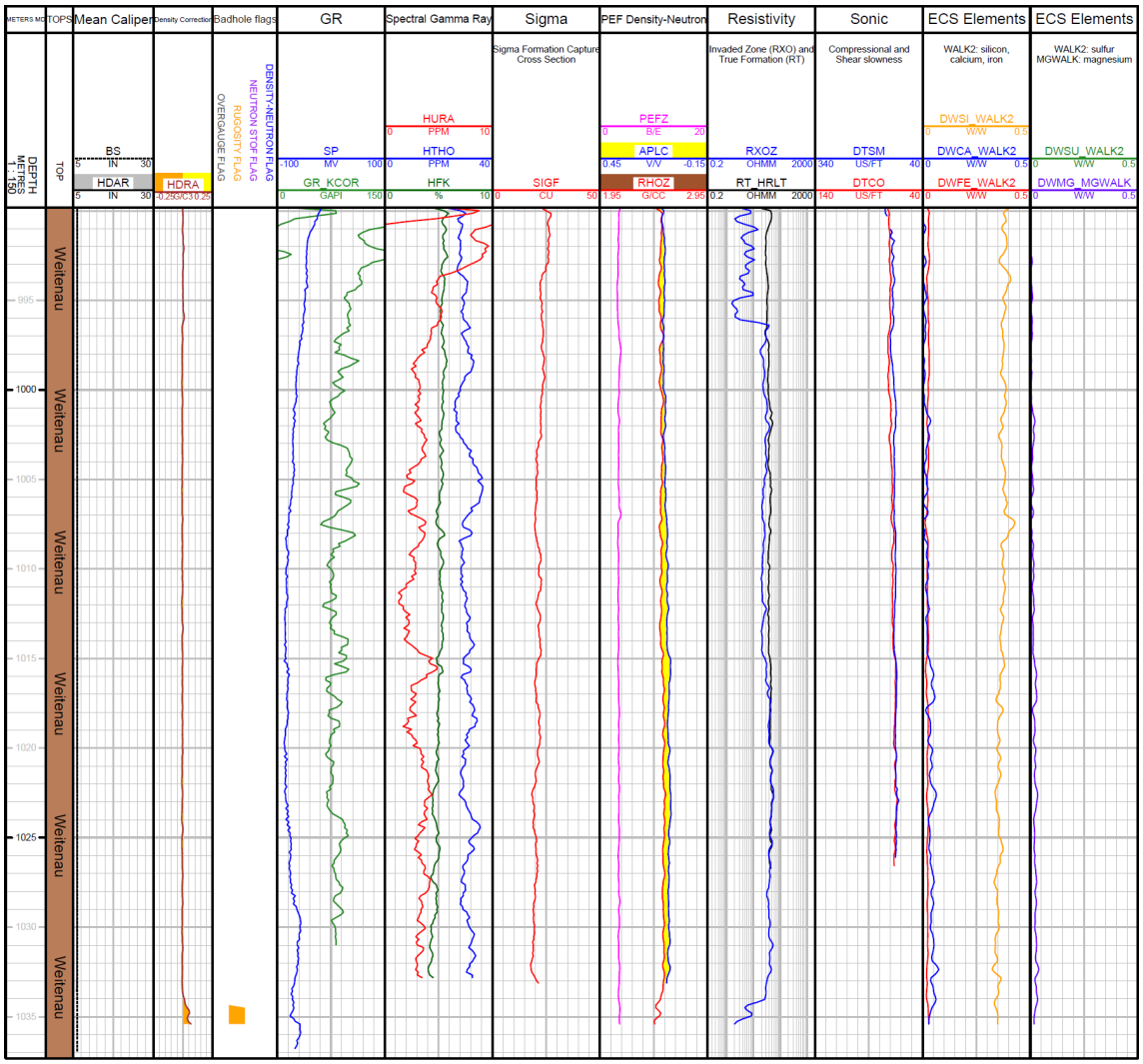

Fig. 3-11: Main logs of the composite dataset in the Weitenau Formation

3.5 Post-completion mud temperature

A temperature log was acquired by Schlumberger post-completion (in cased hole) on 10.08.2021 (Run 5.2.1) to measure the undisturbed temperature of the mud after the last mud circulation on 30.11.2020. Temperature was measured using the EMS tool, which has an accuracy of ± 1 °C and resolution of 0.1 °C. In Fig. 3-12, only the downlog from Run 5.2.1 is plotted as it is believed to be the most representative of the formation temperature. It was acquired at a slow rate of 193 m/hr to avoid mixing of the hydrostatic mud column. Maximum temperature of 49.15 °C was recorded from 869.44 m MD to TD, while the minimum of 16.63 °C was at 199.80 m MD. In the Opalinus Clay, the temperature varies between 29.86 and 38.24 °C and the average geothermal gradient is $\Delta T/\Delta D$ = 0.069 °C/m. The overall temperature gradient is higher in the clay-rich units of the Dogger compared to the calcareous units of Malm and Muschelkalk.

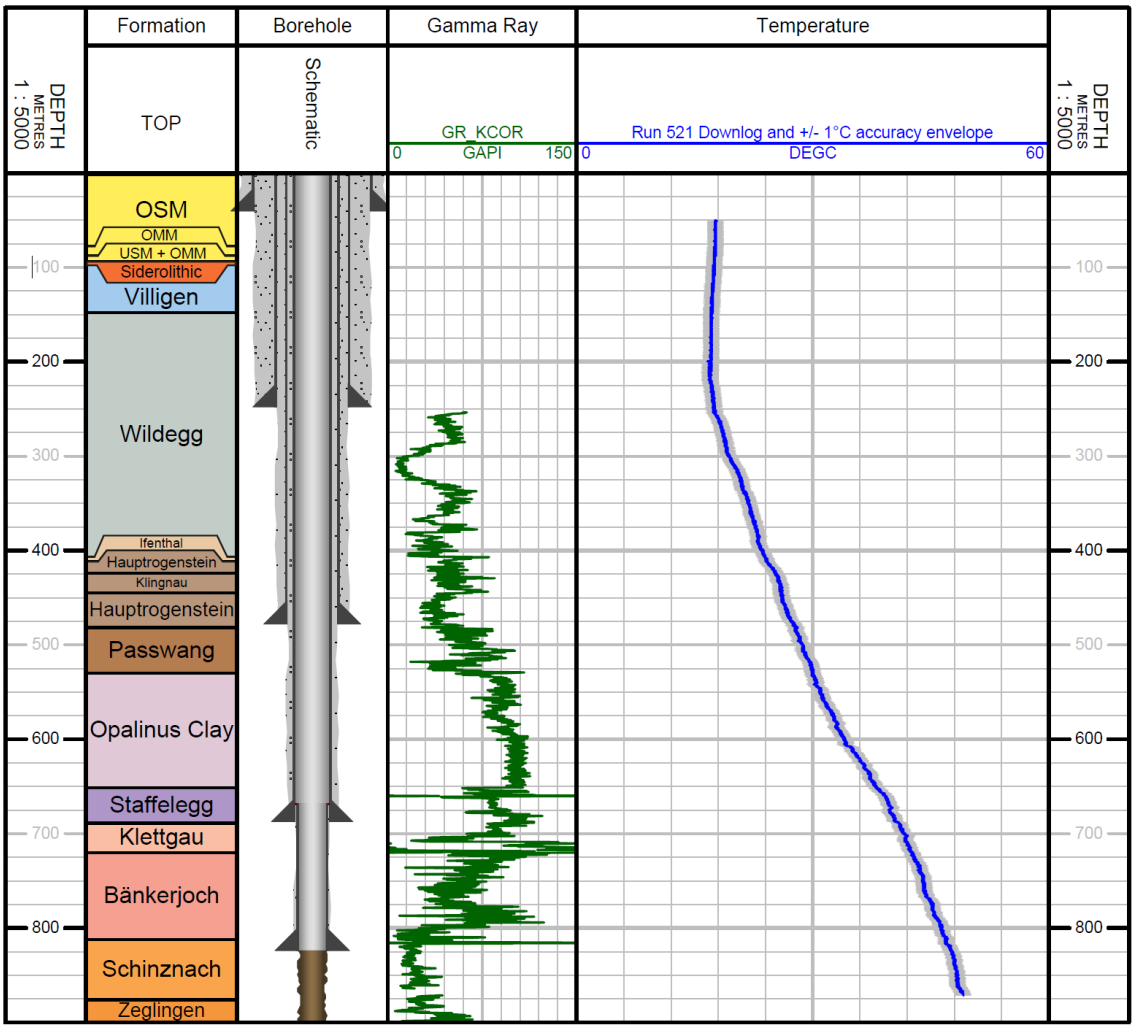

Fig. 3-12: Post-completion temperature log from the downlog pass of Run 5.2.1 (10.08.2021)
A ± 1 °C accuracy envelope is drawn in grey around the temperature log.

4 Borehole Imagery (BHI)

Borehole imaging tools produce high resolution circumferential images of the borehole wall by measuring either resistivity with tool pad contact or ultrasonic velocity. For the BOZ1-1 borehole, SLB's Fullbore Formation MicroImager (FMI) and Ultrasonic Borehole Imager (UBI) were used. The FMI comprises of four pads that measure the formation resistivity via an array of buttons (24 per pad) that are pressed against the borehole wall, providing a vertical resolution of 2.5 mm and 80% coverage in an 8" hole diameter. The UBI has a rotating sub that sends out acoustic pulses to the formation and measures the amplitude and travel time of the returning signals, providing 5 mm vertical resolution and 100% borehole coverage. In general, fractures, faults and bedding are more easily identifiable using the FMI than the UBI as the microresistivity images provide better contrast. However, borehole wall features can be missed if they are located in an area not covered by the tool pad, which is why FMI and UBI images should be used together for image interpretation. In addition, breakouts are typically poorly resolved on microresistivity images because fracturing and spalling associated with these breakouts result in poor contact of the tool pads with the borehole wall.

BHI was used to:

- identify and characterise geological, sedimentological and structural features including bedding, fault planes / zones and fractures
- identify stress-induced borehole phenomena such as tensile drilling-induced fractures and breakouts
- perform core goniometry
- select MHF and PMT testing locations (referred to as stations herein)
- detect and orient fractures induced by MHF stress measurements

For details on the first three uses of BHI, please refer to Dossier V. Only the latter two will be discussed further in the present Dossier.

The BHI, that was acquired pre-MHF, was quality-controlled (QCed), processed and interpreted by NiMBUC Geoscience in a limited amount of time (i.e. rush processing and basic quicklook interpretation). The aim of this quicklook interpretation was to provide a general and quick picture of existing borehole / rock heterogeneities (breakouts, natural and induced fractures etc.) for the selection of MHF and PMT stations immediately after BHI log acquisition and prior to MHF / PMT. In Fig. 4-1, the workflow used by NiMBUC Geoscience is described. Final processed and spliced pre-MHF image logs are included in Dossier V (Appendix B and Appendix C).

The post-MHF imagery underwent a similar workflow to the pre-MHF imagery, however, only the intervals that underwent stress testing were interpreted. These will be detailed in a future MHF interpretation report. To determine whether fractures were generated or enhanced (opened further), the pre- and post-MHF imagery was plotted side-by-side, along with the MHF test interval, packer positions and core photographs (see Appendix D).

Step 1: Image QC	
Depth matching	Correlate high resolution image with reference GR
Caliper check	Verify calibration with casing ID, identify if borehole conditions could affect image quality (washouts, mud cake etc.)
Hardware check	Identify if downhole equipment performance indicators such as gain and voltage supply are consistent
Orientation check	Ensure orientation data are in agreement with borehole azimuth and deviation from independent survey
Accelerometer check	Accelerometer measurement should be consistent with earth's gravity (1 g = 9.81 ± 0.03 m/s^2)
Magnetometer check	Magnetometer consistent with theoretical magnetic field strength at location, X-Y magnetometers behave complementary, QC magnetic declination parameters input
Tool movement check	Identification of any stick and pull events using tension and accelerometer measurements
Acquisition check	Verify frame time and cable speed control
Borehole image check	Identification of dead buttons or pads and any casing interference

Step 2: Image processing	
Basic image generation	Azimuthal orientation of images to true or grid north
	Merging of individual tool run passes
	Splicing of data between drilling sections
	If required, invert images to ensure per industry standards that low value = low resistivity and high value = high resistivity
	If required, correct offsets between pad images
	Bad button detection and correction
Image equalisation and normalisation	Static normalisation involving selecting the normalisation distribution (uniform/Gaussian), equalisation strength, high/low cut-offs for equalisation etc.
	Dynamic normalisation to enhance local contrasts highlighting features in a selected sliding window of a few metres

Step 3: Basic interpretation	
Manual picking of features directly from the processed image in accordance with Nagra classification scheme detailed here	Drilling-induced fractures
	Borehole breakouts
	Bedding
	Fractures (conductive, partially conductive, resistive, partially resistive, faint trace)
	Faults (conductive, partially conductive, resistive, partially resistive, faint)

Fig. 4-1: Borehole image processing workflow

5 Micro-hydraulic Fracturing (MHF)

5.1 Introduction and objectives

A series of stress measurements was performed in the BOZ1-1 borehole using the Micro-hydraulic Fracturing (MHF) technique. MHF testing in boreholes is the only direct method available for measuring rock stress magnitude at great depth. An overview of the methodology can be found in Haimson (1993), Desroches & Kurkjian (1999) and Haimson & Cornet (2003) and references therein. Recent updates on the methodology, some of which having been specifically designed for this project, can be found in Desroches et al. (2021a, 2021b).

The objectives of the testing programme are to acquire data to:

- provide estimates of the in situ stress state in the Opalinus Clay and adjacent rock formations, and
- provide calibration points for mechanical earth models (MEM) of the rock mass (1D, 3D). See Bérard & Prioul (2016) for an overview of mechanical earth models and Plumb et al. (2000) for a definition of an MEM.

Key features include:

- Core images and BHI (FMI and UBI) were used to select the appropriate test depths closest to where geomechanical lab test samples were taken.
- The MHF protocol that was used, was tailored in real-time to bracket the far-field closure stress as closely as possible.
- Post-MHF imaging logs were run to determine the trace of the newly created fractures, enabling better allocation of the MHF closure stress to a principal stress direction.
- Sleeve fracturing was regularly used to focus the test on the desired interval; sleeve reopening was used to allow the estimation of the maximum horizontal stress when the MHF tests yielded an estimate of the minimum horizontal stress.

5.2 MHF theory

MHF tests an interval of approximately 1 m which is sealed above and below by packers that are approximately 0.5 m in length (exact dimensions are dependent on the configuration of the tool string). A schematic, showing the first two hydraulic fracturing cycles for a typical MHF test, is presented in Fig. 5-1. Once the interval is sealed, a micro-hydraulic fracturing cycle begins with pressurising the interval (1st step) until fracture initiation. Fluid keeps being injected to extend the micro-hydraulic fracture into the formation by a couple of decimetres (2nd step). Injection is then stopped to allow fracture closure, and pressure fall-off is observed (3rd step). Similar steps are repeated to further extend and refine the testing of the micro-hydraulic fracture until the test is deemed satisfactory. Tests performed in this borehole have included more complex testing techniques as reported in Desroches et al. (2021a).

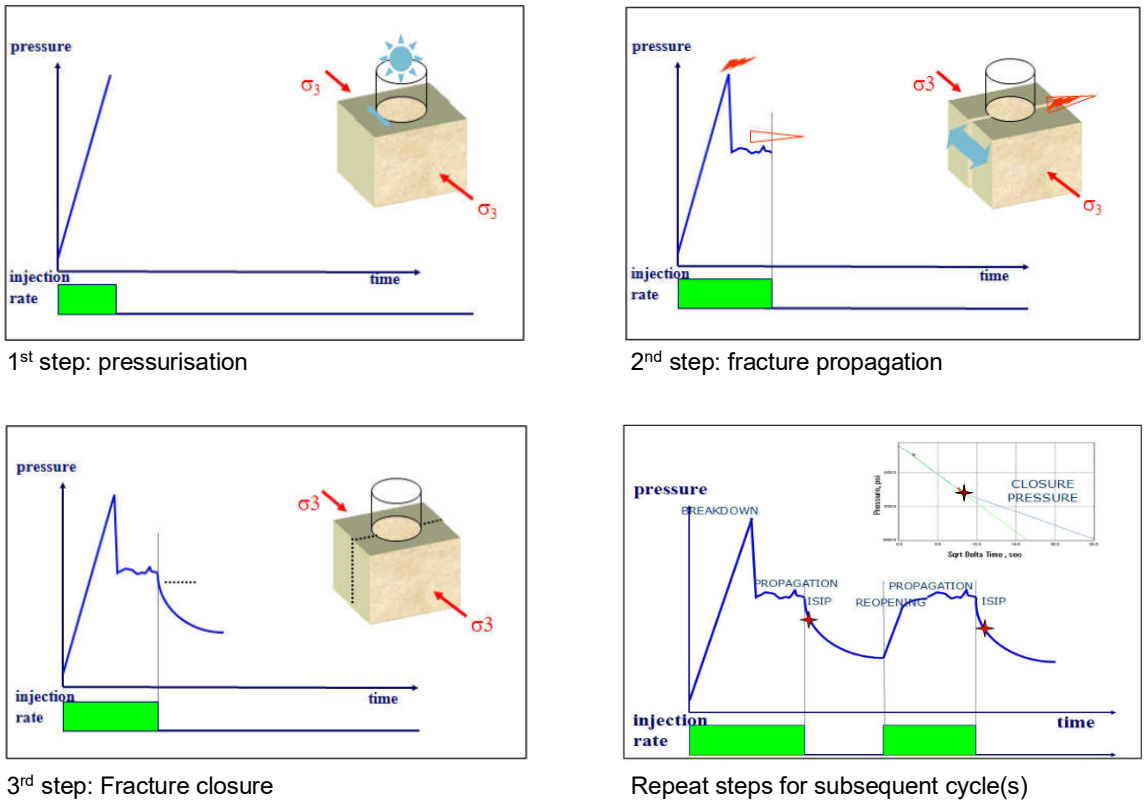

Fig. 5-1: Schematic showing the response of the interval pressure to fluid injection in the interval as a function of time during an MHF test and associated formation response (courtesy of SLB)

5.3 Test protocol

Each test consisted of a succession of steps according to the general test procedure described in Desroches & Kurkjian (1999), Haimson & Cornet (2003) and Wileveau et al. (2007). Although a general procedure was followed for each test, the steps were tailored in real-time to ensure that the pressure records provided the best possible estimate for closure stress (see Desroches et al. 2021b). As a result, the number of steps and their nature varied from test to test.

The steps undertaken during a stress test were as follows:

- Depth correlation: validate the cable depth by comparing GR logs with the reference GR log of the borehole.
- Sleeve fracturing: this step is analogous to sleeve reopening (see below) but performed prior to the micro-hydraulic fracturing operation. The single packer is placed in front of the desired depth and applies pressure to focus the initiation of a longitudinal fracture at the desired interval. Note that this part of the sequence is not carried out if a pre-existing fracture (natural or drilling-induced or -enhanced) is present in the test interval.
- Packer inflation and leak-off test: the straddle packer is positioned so that the centre of the interval is in front of the desired depth. Packers are inflated to a differential pressure of 300 to 500 psi and the integrity of the seal is observed. The integrity of the seal is further validated by a short injection into the interval.

- Breakdown cycle (steps 1 to 3 in Fig. 5-1): the first cycle in a test during which a hydraulic fracture is propagated was counted as a breakdown cycle (even if technically there is no breakdown, e.g. because a pre-existing drilling-induced fracture was tested). To ensure that cycles are not counted more than once, there was only one breakdown cycle per test. Whether it starts with a step-rate test or ends with a slamback / rebound test (see below), it is still only counted as one breakdown cycle.
- Reopening cycle: any subsequent injection / shut-in cycle during which a fracture is propagated and that neither starts with a step-rate test nor ends with a slamback / rebound test (see below) is counted as a reopening cycle.
- Slamback / rebound test: at the end of an injection cycle during which a fracture was propagated (but not for the first time), the interval is quickly opened and closed for a fast depressurisation, and pressure rebounds from a value close to borehole hydrostatic pressure. The slamback occurs immediately after the injection stopped, and the rebound is observed until a plateau is reached. If the injection cycle starts with a step-rate test, it is only counted as a step-rate test and not as a slamback / rebound test.
- A new procedure ('forced closure') was introduced in the BOZ1-1 borehole. Because it also involves withdrawing fluid from the interval, cycles with forced closure were not counted separately but were also counted as S/R tests.
- Step-rate test: an injection cycle during which the rate was increased (or decreased) in steps with at least three different flow rates during the cycle is called a step-rate test. An injection cycle during which the rate was only changed once cannot be counted as a step-rate test because it does not allow a step-rate interpretation.
- Sleeve reopening: the single packer is moved in front of the previously tested interval and pressure is applied with the aim of detecting and reopening the fracture created during the micro-hydraulic fracturing cycles.

In Fig. 5-2, an example of the pressure record for a MHF test performed in the BOZ1-1 borehole is presented (Station 1-3, Run 2.6.3). Fig. 5-2a shows the pressure in the interval as well as the inflate pressure in the packers, Fig. 5-2b the fluid injection rate as a function of time, Fig. 5-2c the injected volume as a function of time and Fig. 5-2d, also called a reconciliation plot, displays the characteristic pressures estimated for all cycles for which a fracture was created / tested. For this test, there were a total of 5 MHF cycles, labeled 8 to 18. The first cycles are not analysed as they correspond to the packer inflation and leak-off test. Fracture breakdown took place during cycle 8, which corresponds to the breakdown / propagation cycle depicted in the theory schematic (Fig. 5-1). Cycles 10, 12 and 18 are reopening tests, cycles 14 and 16 are step-rate tests (cycles 9, 11, 13, 15 and 17 are absent from interpretation because they are packer inflation cycles). A slamback / rebound test was performed at the end of cycles 14 and 18. The characteristic pressures presented in Fig. 5-2d reflect the stress acting on the fracture: they validate the creation of a hydraulic fracture and exhibit a rather constant behaviour, especially for the last 3 cycles, which supports that an estimate of the far-field stress can be obtained from the test.

The raw MHF pressure-time and reconciliation plots for all tests conducted in the BOZ1-1 borehole are included in Appendix E. In Tab. 5-1, a summary of the steps taken for each MHF station is given, along with the associated formation / unit that was tested. Stations are presented in operational order.

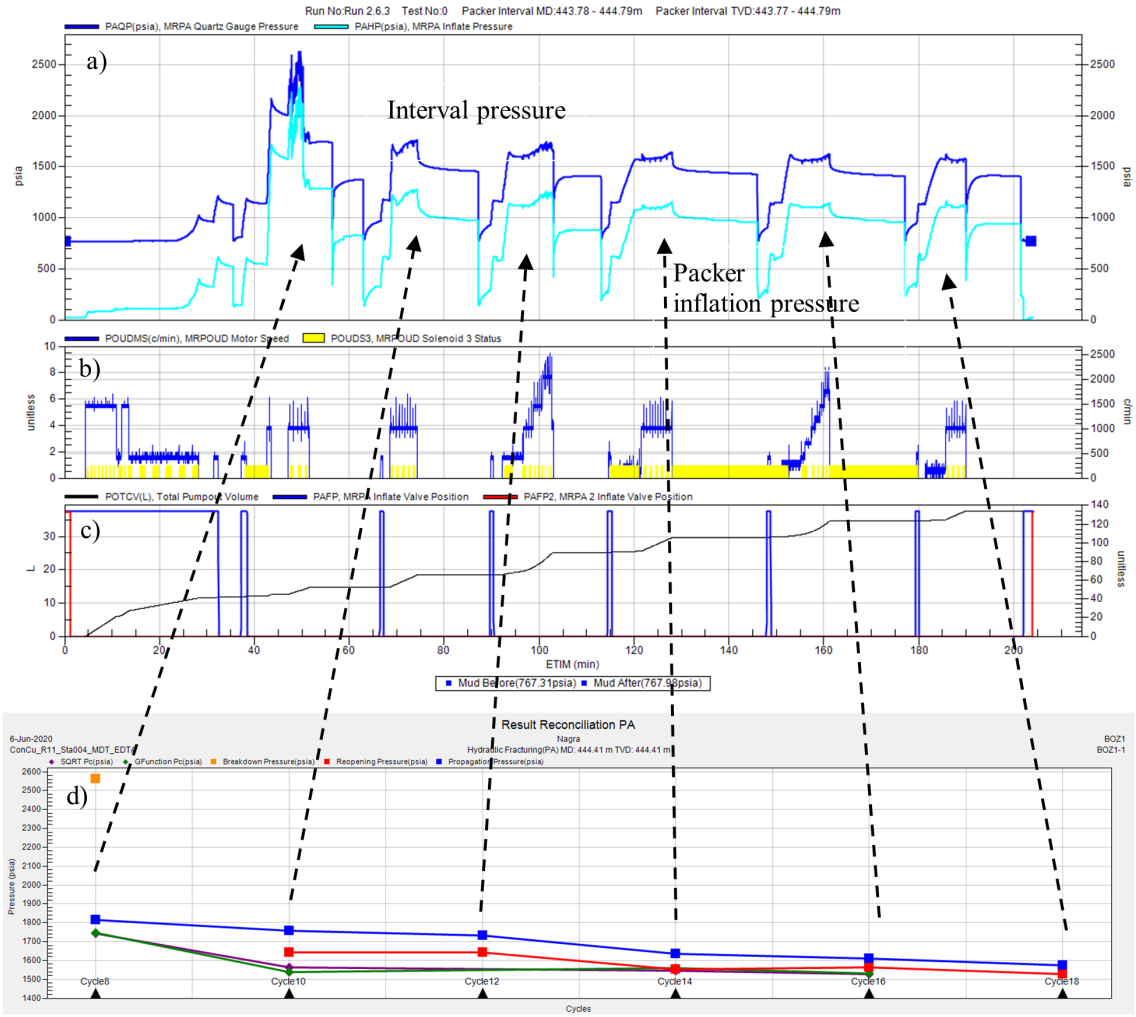

Fig. 5-2: Example of pressure record for MHF test from BOZ1-1 (Station 1-3, Run 2.6.3)
Pc stands for closure pressure, ISIP stands for Instantaneous Shut-in Pressure.

Tab. 5-1: Summary of MHF station locations and operations carried out for each section of the BOZ1-1 borehole

Phase / Section	**Station**	**Formation / unit**	**Middle interval depth** [m]	**Sleeve fracturing cycles**	**Break-down cycles**	**Reopening cycles**	**Slamback / rebound tests**	**Step-rate tests**	**Sleeve reopening cycles**
II (Runs 2.6.3 to 2.6.5)	1-3	Klingnau Fm.	444.3	2	1	2	1	2	2
	1-4	Hauptrogenstein	448.8	2	0	-	-	-	-
	1-5	Klingnau Fm.	440.95	2	1	4	0	2	2
	2-1	Wildegg Fm.	374.7	2 x 2	1	3	1	2	2
	2-6	Wildegg Fm.	344.2	2	1	1	1	2	3
	3-1	Wildegg Fm.	397.35	6	1	3	0	2	2
	3-2a	Wildegg Fm.	400.8	0	1	3	0	1	2
	4-1	Ifenthal Fm.	409.2	2	1	2	0	1	-
	4-1a	Ifenthal Fm.	408.7	0	1	2	2	0	2
	2-3	Wildegg Fm.	289.7	2	1	2	2	2	2
III (Run 3.3.3)	1-1	Staffelegg Fm.	667	2	1	2	0	2	2
	2-1	Opalinus Clay	645.45	2	1	3	0	2	2
	2-3	Opalinus Clay	533.75	2	1	3	0	2	2
	3-1	Passwang Fm.	512.8	2	1	3	0	2	2
	2-2	Opalinus Clay	634.5	2	1	1	0	2	2
	2-5	Opalinus Clay	550.6	2	1	3	0	2	2
	2-4	Opalinus Clay	584.3	2	1	2	1	2	2
IV (Run 4.4.2)	1-1	Schinznach Fm.	825.45	4	1	4	0	2	2
	2-1	Bänkerjoch Fm.	806.2	2	0	-	-	-	-
	2-2	Bänkerjoch Fm.	801.1	2	1	2	1	2	2
	3-1	Klettgau Fm.	718.7	2	1	3	0	2	2
	3-2	Klettgau Fm.	717.4	2	1	1	1	2	2
	1-2	Schinznach Fm.	828.5	2	1	2	0	2	2
	2-5	Bänkerjoch Fm.	787.2	2	1	3	2	3	2
V (Runs 5.1.10 & 5.1.11)	1-1	Dinkelberg Fm.	974.6	2	1	2	0	1	-
	1-2	Kaiseraugst Fm.	966.5	3	1	3	0	2	2
	2-1	Schinznach Fm.	841.4	1	1	1	0	1	2
	3-1	Zeglingen Fm.	903.9	5	1	2	1	2	-
	3-2	Zeglingen Fm.	911.2	2	1	1	1	2	2
	5-1	Weitenau Fm.	1'002.4	0	1 (but lost seal)	-	-	-	-
	4-2	Kaiseraugst Fm.	939.35	0	1	2	2	2	2

5.4 MHF results

31 tests were attempted, with 26 of them being successful, from the Wildegg Formation (148 m) down to the Weitenau Formation (1'037.39 m). Tests without the ability to breakdown the formation or with an inability to maintain a high-pressure seal were deemed unsuccessful. Any other test where a closure stress could be estimated was deemed successful.

Tab. 5-2 presents a quicklook interpretation of the MHF results which includes the 'breakdown pressure', the closure stress range and associated comments. The 'breakdown pressure' is taken as the maximum pressure reached during the first hydraulic fracturing cycle. A classical breakdown pressure interpretation should not be applied to these pressure values because sleeve fracturing was performed prior to hydraulic fracturing. Recorded 'breakdown pressures' are therefore technically reopening pressures. The closure stress acts normal to the fracture surface. Its range was determined from the pressure records and expressed with a lower and an upper bound.

Fig. 5-3 plots the closure stress ranges from the quicklook analysis as a function of depth together with the overburden vertical stress (Sv), estimated from integration of the density logs over depth, and the maximum pressures measured during the formation integrity tests (FIT).

Quicklook analysis of the post-MHF borehole imagery showed that new or enhanced features (longitudinal) could be observed at successful station locations. Conversely, in unsuccessful tests, no new feature could be observed. Fig. 5-4 presents the pre- and post-MHF images for Station 1-4 (Runs 2.6.3). New fracture segments induced by the MHF test are highlighted by black boxes on the rightmost track. Note that there were no pre-existing fractures on the pre-MHF images. The MHF test led to the creation of slightly inclined conductive fractures at the wellbore, which cover the entire length of the straddle packer arrangement (and even extend away from it). The azimuth of these new fracture traces indicates the azimuth of the maximum horizontal stress. A comparison of all the pre- and post-MHF borehole images is included in Appendix D.

Interpretation of sleeve fracturing / sleeve reopening tests was not performed as part of the acquisition programme and is not included in this report.

Tab. 5-2: Quicklook interpretation of MHF results for BOZ1-1 borehole

Section Run Diameter	**Station**	**Formation**	**Depth** [m]	**Breakdown pressure** [MPa]	**Closure stress range** [MPa]	**Comments**
II Runs 2.6.3 to 2.6.5 8½" bit size	2-3	Wildegg Fm.	289.7	10.83	6.15 – 6.76	S_{hmin} likely
	2-6	Wildegg Fm.	344.2	10.98	8.35 – 9.30	S_{hmin} or S_V?
	2-1	Wildegg Fm.	374.7	13.72	8.27 – 11.00	Higher than anticipated
	3-1	Wildegg Fm.	397.35	15.71	9.30 – 10.05	S_{hmin} or S_V?
	3-2a	Wildegg Fm.	400.8	14.45	9.10 – 10.09	HTPF: larger than minimum stress
	4-1a	Ifenthal Fm.	408.7	14.30	6.20 – 8.25	S_{hmin} likely
	4-1	Ifenthal Fm.	409.2	16.58*	n/a	No breakdown – moved up by 0.5m
	1-5	Klingnau Fm.	440.95	16.47	8.82 – 12.25	S_{hmin} likely, higher than anticipated
	1-3	Klingnau Fm.	444.3	17.67	9.72 – 11.20	S_{hmin} likely, higher than anticipated
	1-4	Hauptrogenstein	448.8	24.13*	n/a	No breakdown
III Run 3.3.3 8½" bit size	3-1	Passwang Fm.	512.8	15.13	11.35 – 13.3	Likely S_{hmin}, possibly S_V
	2-3	Opalinus Clay	533.75	30.18	9.65 – 13.8	S_{hmin} likely
	2-5	Opalinus Clay	550.6	27.40	9.65 – 11.75	S_{hmin} likely
	2-4	Opalinus Clay	584.3	17.63	11.25 – 12.05	S_{hmin} likely
	2-2	Opalinus Clay	634.5	20.50	11.24 – 11.9	S_{hmin} likely
	2-1	Opalinus Clay	645.45	16.75	12.4 – 13.6	S_{hmin} likely
	1-1	Staffelegg Fm.	667	28.31	12.7 – 13.55	S_{hmin} likely
IV Run 4.4.2 8½" bit size	3-2	Klettgau Fm.	717.4	18.96	12.75 – 13.80	S_{hmin} likely
	3-1	Klettgau Fm.	718.7	20.55	11.35 – 13.45	S_{hmin} likely
	2-5	Bänkerjoch Fm.	787.2	33.89	17.2 – 21.35	S_{hmin} likely
	2-2	Bänkerjoch Fm.	801.1	28.91	18.6 – 22.1	S_{hmin} likely
	2-1	Bänkerjoch Fm.	806.2	43.78*	n/a	No breakdown
	1-1	Schinznach Fm.	825.45	26.37	10.9 – 15.15	S_{hmin} likely
	1-2	Schinznach Fm.	828.5	28.19	11.35 – 15.18	S_{hmin} likely
V Runs 5.1.10 to 5.1.11 6⅜" bit size	2-1	Schinznach Fm.	841.4	19.79	10.7 – 14.5	S_{hmin} likely
	3-1	Zeglingen Fm.	903.9	41.27	30 – 34.8	Likely S_{hmin} but larger than anticipated
	3-2	Zeglingen Fm.	911.2	39.15	20.0 – 23.0	S_{hmin} likely, S_V possible
	4-2	Kaiseraugst Fm.	939.35	22.07	14.45 – 15.87	S_{hmin} likely
	1-2	Kaiseraugst Fm.	966.5	26.90	17.9 – 20.7	S_{hmin} likely
	1-1	Dinkelberg Fm.	974.6	27.04*	n/a	No breakdown
	5-1	Weitenau Fm.	1'002.4	17.03*	n/a	No breakdown
Total number of tests						31
Total number of successful tests						26
Success rate (actual vs. attempted) & (actual vs. desired from initial plan)						84% & 124%

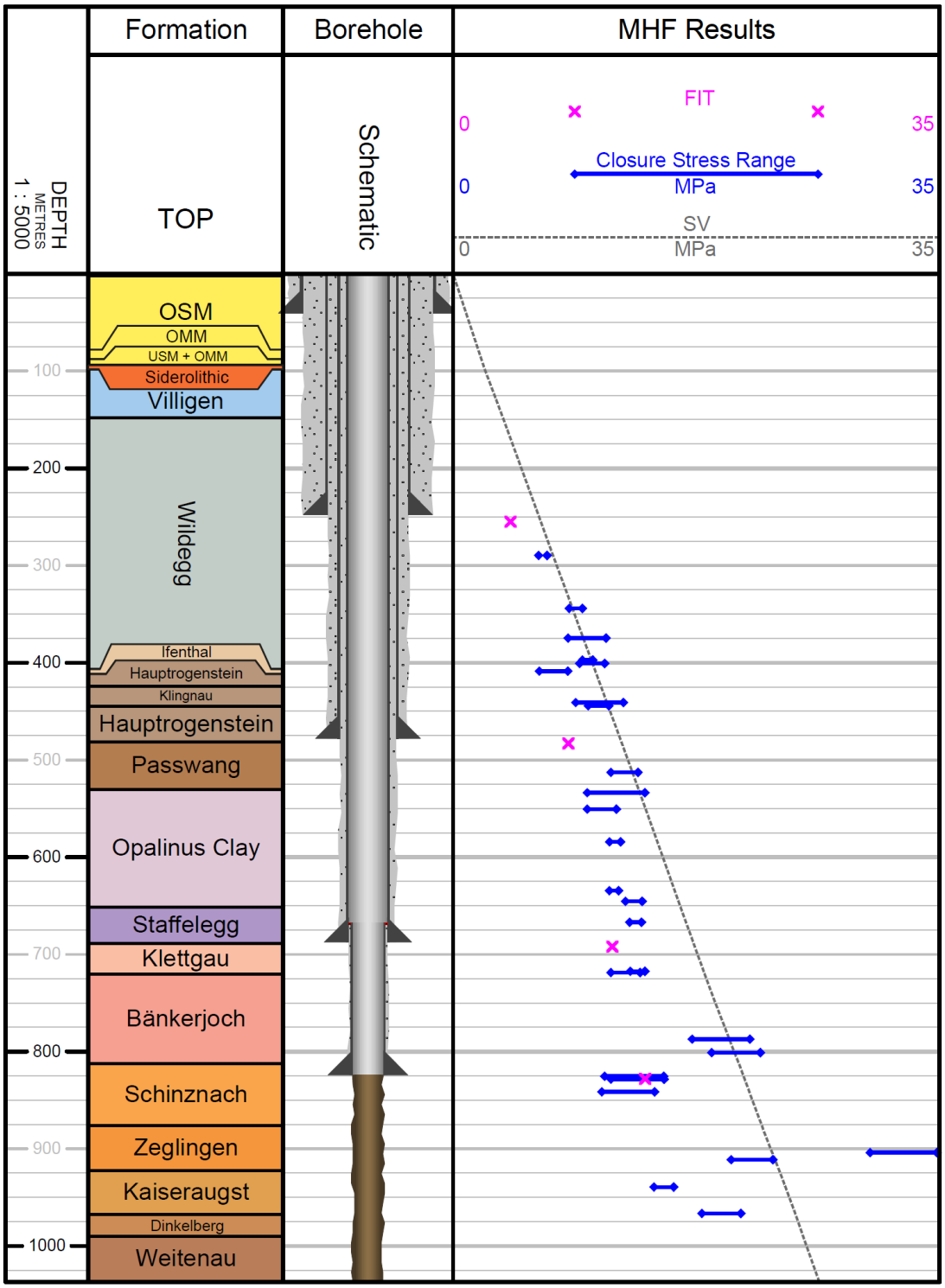

Fig. 5-3: Comparison of the quicklook closure stress range obtained from the BOZ1-1 MHF tests with the overburden vertical stress (Sv) from the integration of density over depth and the maximum pressures attained during the formation integrity tests (FIT)

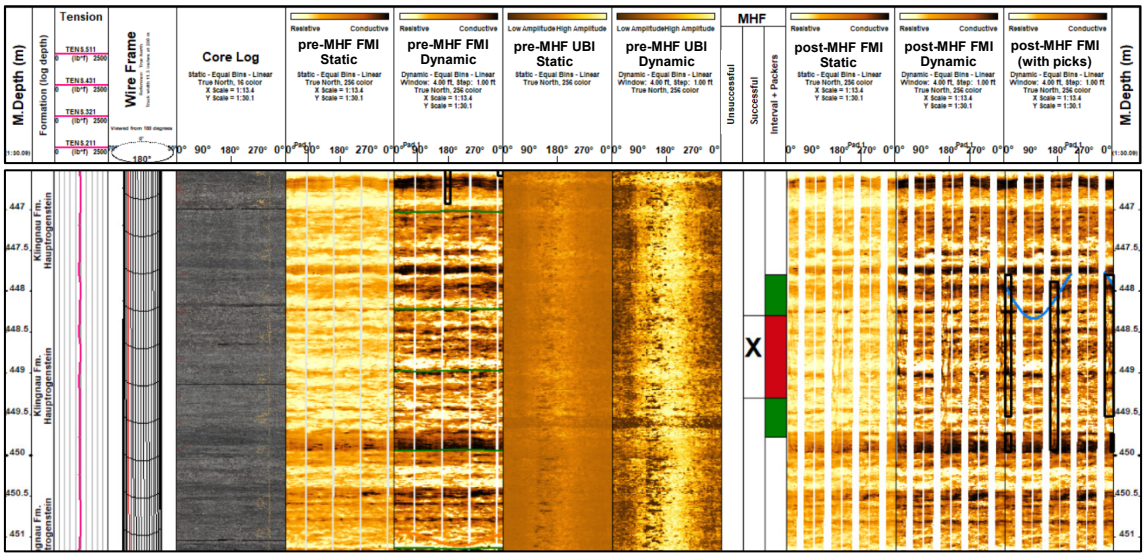

Fig. 5-4: Example of pre- vs. post-MHF images from BOZ1-1 (Station 1-4 from run 2.6.3, Section II)

Pre- and post-MHF images are presented on the left and right of the MHF columns, respectively.

New fracture traces created by the MHF test are shown in the black boxes picked by NiMBUC Geoscience on the post-FMI dynamic image.

6 Pressure-meter Testing (PMT)

6.1 Introduction and objectives

PMT tests were conducted to estimate the in situ shear modulus by testing a larger volume of rock than is possible during laboratory tests of core samples and at larger strains than during sonic logging. Testing was performed during MHF operations using the single packer module that is used to perform sleeve fracturing and sleeve reopening as discussed in Chapter 5. The main aim of the BOZ1-1 PMT was to select the best possible combination of hardware / test protocol for comparison with future dilatometer tests which will be performed in the STA2-1, STA3-1 and BAC1-1 boreholes.

To be able to interpret a PMT test, a calibration test is required that is carried out in either a casing joint, a formation of known stiffness, or a formation that is stiffer than the tool. Different combinations of calibration tests have been explored during the BOZ1-1 PMT campaign.

6.2 Test protocol

A series of cycles with increasing maximum pressure were conducted to avoid creating a tensile fracture during the first cycle.

All tests were initiated with a packer inflation procedure, the aim of which was to ease the packer into place at the station location. Different procedures were explored to optimize both operational time and contact between the packer and the formation.

After packer inflation was complete, a combination of partial or full deflation protocols was undertaken. A summary of the different protocols that were undertaken is presented below. They are all variations of what is presented in the ASTM Standard D8359-20, "Standard test method for determining in situ rock deformation modulus and other associated rock properties using a flexible volumetric dilatometer" (2020).

Note that in the text below "pressure" refers to the packer inflation pressure. The packer inflation pressure is the differential pressure between the hydrostatic pressure in the borehole and the absolute fluid pressure in the packer: it is the pressure difference seen by the packer membrane.

Packer inflation:

- The test procedure may start with an optional full stretch of the packer, inflating to a pressure of 3'000 psi followed by complete packer depressurization.
- The packer is inflated to a pressure of 250 psi; fall-off is observed for 5 min. The packer is then de-pressurised.
- The packer is re-inflated again to a pressure of 250 psi; fall-off is observed for 5 min. The packer is not de-pressurised before the next steps.

Partial deflation protocol

- The packer is inflated to increasing pressure levels, typically in steps of 500 psi (e.g. 1'000 psi, 1'500 psi, 2'000 psi).
- For each inflation cycle, the packer is inflated to the desired level; fall-off is observed for 3 min.

- The packer is then partially deflated into a sample chamber to decrease the pressure by 250 psi to 500 psi.
- The packer is then inflated to the next desired pressure level; fall-off is observed for 3 min followed by partial deflation, until the final desired pressure is reached.

  To ensure that the test samples intact rock, the maximum inflation pressure for the entire test should be lower than the sleeve fracturing breakdown pressure.

Full deflation protocol

- The packer is inflated to increasing pressure levels, typically in steps of 500 psi (e.g. 1'000 psi, 1'500 psi, 2'000 psi).
- For each inflation cycle, the packer is inflated to the desired level; fall-off is observed for 3 min.
- The packer is then deflated down to a pressure level of 30 psi to 50 psi to ensure that full contact between the packer and the borehole is maintained.
- The packer is then inflated to the next desired pressure level; fall-off is observed for 3 min followed by deflation until the final desired pressure is reached.

  To ensure that the test samples intact rock, the maximum inflation pressure for the entire test should be lower than the sleeve fracturing breakdown pressure.

Reduced protocol

The reduced protocol was designed based on experience from previous tests with the aim of performing a faster test before the sleeve fracturing test:

- packer inflation protocol
- inflate to 1'000 psi; wait for 3 min; deflate*
- inflate to 2'000 psi; wait for 3 min; deflate*
- inflate to 3'000 psi; wait for 3 min; deflate*

  * Every packer deflation reduces the inflation pressure to 30 psi to 50 psi if possible.

For PMT dedicated stations, the maximum inflation pressure for the entire test was kept lower than the sleeve fracturing breakdown pressure. In other words, the final inflation pressure of 3'000 psi was not always performed if it meant exceeding the anticipated sleeve breakdown pressure of the formation.

Some PMT tests were integrated with the sleeve fracturing (SF) test. Under these circumstances, the maximum inflation pressure need not be limited as sleeve fracturing cycles follow immediately after the PMT protocol.

6.3 Results

A total of six PMT tests were carried out with different packer types (IPCF-PC-700 – standard 7" packer, Frac12k – very high pressure 7" packer, SST-5 – high pressure 5" packer), pump types (standard or constant displacement) and displacement units (high pressure displacement unit [HPDU], extra-high-pressure displacement unit [XPDU]), as well as different protocol combinations. Three of these were dedicated PMT tests and the other three PMT tests that were integrated into a SF test. In addition, six calibration tests were performed, five in casing (at different depths and both before and after the PMT tests) and one in a very stiff formation. Details of the PMT related operations are reported in Tab. 6-1. Note that, for comparison with MHF tests, the pressures that are reported in the description of the protocol are "absolute" pressures, i.e. corresponding to the fluid pressure in the packer – not the inflation or differential pressure.

During Runs 2.6.4 and 2.6.5, two protocols were explored, one where the packer was only partially depressurized between two inflation cycles ("partial deflation protocol") and the other where the packer was fully depressurized between two inflation cycles ("full deflation protocol").

During Run 3.3.3, the comparison between partial and full deflation of the packer was further explored, resulting in the abandonment of the partial deflation protocol.

During Run 4.4.2, the protocol included fully stretching the packer prior to starting the PMT cycles. The depth and timing of the casing calibration tests was also explored. A different packer type was also tested.

During Run 5.1.11, the reduced protocol was explored and the casing calibration test replaced with a test in a very stiff formation. A different packer was also tested because of the reduced borehole diameter.

Tab. 6-1: PMT details

Section Run Diameter	**Formation**	**Middle packer depth** [m]	**Packer type**	**Pump type Displacement unit**	**Protocol adjustments**
II Runs 2.6.4 and 2.6.5 8½" bit size	Casing test	Surface	IPCF-PC-700	Standard pump HPDU	Partial deflation protocol, 7 cycles from 750 to 3'000 psi absolute pressure after packer inflation.
	Wildegg Fm.	337.50	IPCF-PC-700	Standard pump HPDU	Dedicated PMT station. Partial deflation protocol, 7 cycles from 1'300 psi to 3'500 psi absolute pressure after packer inflation.
	Opalinus Clay	648.65 (dedicated PMT station)	IPCF-PC-700	Standard pump HPDU	Partial deflation protocol. After packer inflation: 5 cycles from 1'900 to 2'500 psi absolute pressure, partial deflation protocol; followed by 4 cycles from 2'100 to 3'600 psi absolute pressure, full deflation protocol.
IV Run 4.4.2 8½" bit size	Casing test – prior to PMT tests	637.6	Frac12k	Standard pump XPDU	Full packer stretch prior to packer inflation. Full deflation protocol, 5 cycles from 1'860 to 4'100 psi absolute pressure after packer inflation.
	Klettgau Fm.	705.4 (dedicated PMT station)	Frac12k	Standard pump XPDU	Full packer stretch to packer inflation. Full deflation protocol, 6 cycles from 2'000 to 4'200 psi absolute pressure after packer inflation.
	Bänkerjoch Fm. anhydrite	806.2 (PMT prior to SF)	Frac12k	Standard pump XPDU	Full packer stretch prior to packer inflation. Full deflation protocol, 6 cycles from 2'250 to 4'600 psi absolute pressure after packer inflation.
	Casing test after PMT tests	637.6	Frac12k	Standard pump XPDU	Full packer stretch prior to packer inflation. Full deflation protocol, 6 cycles from 1'860 to 4'100 psi absolute pressure after packer inflation.
	Casing test – final	114.9	Frac12k	Standard pump XPDU	Full stretch to 3'000 psi prior to packer inflation. Full deflation protocol, 6 cycles from 1'000 to 3'250 psi.
V Run 5.1.11 6⅜" bit size	Zeglingen Fm.	903.9 (PMT prior to SF)	SST-5	Constant displacement pump XPDU	Reduced protocol: full deflation, a total of 5 cycles from 2'500 to 6'900 psi absolute pressure after packer inflation. The first 3 cycles are attributed to PMT and the last 2 cycles to SF.

An example of a pressure record from PMT for the reduced protocol integrated with a sleeve fracturing test is presented in Fig. 6-1. First, the packers were inflated to a low inflation pressure twice, to ease their position against the borehole wall as per the inflation protocol described earlier. Three inflation cycles were then performed up to differential pressures of 1'000 psi, 2'000 psi and 3'000 psi, respectively, with full packer deflation in between. These three cycles were then followed by regular SF cycles without moving the tool.

An example of a possible interpretation methodology is presented in ASTM D8359-20 (2020). Interpretation of the PMT is being performed separately by Schlumberger as part of a special project with Nagra and further results are therefore not reported here. In particular, refinement of results in consideration of the calibration tests is still under investigation. Preliminary results have been presented in Elkhoury et al. (2022), where the shear modulus for the Klettgau formation at 705.4m was evaluated to be 8.8±1.3 GPa.

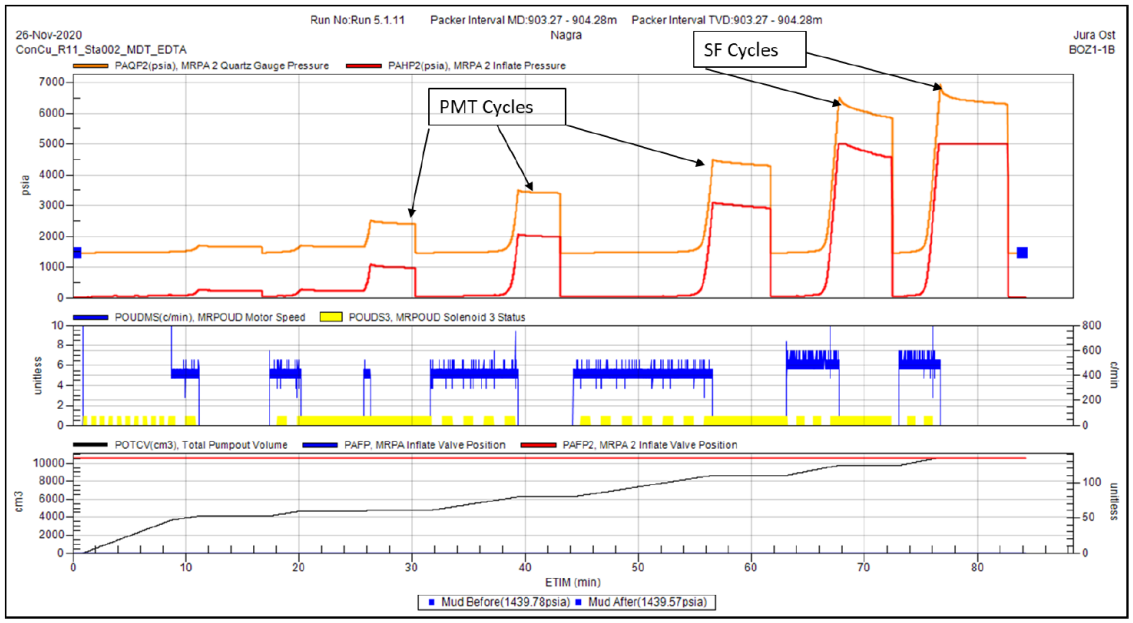

Fig. 6-1: Time summary plot for PMT-SF operation carried out before MHF Station 3-1 (run 5.1.11)

Top plot: packer inflation pressure (red) and packer absolute pressure (orange) – the difference between the two is the borehole hydrostatic pressure; middle plot: pump speed (blue) and piston direction (yellow / white); bottom plot: total injected volume (black).

7 References

ASTM D8359-20 (2020): Standard Test Method for Determining the In Situ Rock Deformation Modulus and Other Associated Rock Properties Using a Flexible Volumetric Dilatometer. DOT:10.1520/D8359-20.

Bérard, T. & Prioul, R. (2016): Mechanical Earth Model. Oilfield Review: The Defining Series, https://www.slb.com/resource-library/oilfield-review/defining-series/defining-mem

Desroches, J. & Kurkjian, A.L. (1999): Applications of wireline stress measurements. Paper SPE-58086, SPE Reservoir Evaluation & Engineering 2/5, 451-461. DOI:10.2118/ 58086-PA.

Desroches, J., Peyret, E., Gisolf, A. Wilcox, A., Di Giovanni, M., Schram de Jong, A., Sepehri, S., Garrard, R. & Giger, S. (2021a): Stress measurement campaign in scientific deep boreholes: Focus on tool and methods. SPWLA Paper #2021-056 presented at the SPWLA 62nd Annual Logging Symposium, May 17-20 2021.

Desroches, J., Peyret, E., Gisolf, A., Wilcox, A., di Giovanni, M., Schram de Jong, A., Milos, B., Gonus, J., Bailey, E., Sepehri, S., Garitte, B., Garrard, R. & Giger, S. (2021b): Stress-Measurement Campaign in Scientific Deep Boreholes: From Planning to Interpretation. ARMA-2-21-1928 presented at the 55th U.S. Rock Mechanics/Geomechanics Symposium, Virtual, June 2021.

Elkhoury, J.E., Elias, Q.K., Prioul, R., Peyret, E., Wilcox, E., di Giovanni, M., van der Hulst, T., Bérard, T., Desroches, J., Garrard, R. and Giger, S. (2022): The first pressuremeter testing campaign in deep boreholes on wireline formation testers. ARMA 22-0698 to be presented at 56th U.S. Rock Mechanics/Geomechanics Symposium, Santa Fe, NM, USA, June 2022.

Haimson, B.C. (1993): The hydraulic fracturing method of stress measurement: Theory and practice. Chapter 14 *in:* Hudson, J. (ed.): Comprehensive Rock Engineering 3, 395-412, Pergamon Press. DOI: 10.1016/B978-0-08-042066-0.500215.

Haimson, B.C. & Cornet, F.H. (2003): ISRM suggested methods for rock stress estimation – Part 3: Hydraulic fracturing (HF) and/or hydraulic testing of pre-existing fractures (HTPF). International Journal Rock Mechanics and Mining Sciences 40/7-8, 1011-1020. DOI: 10.1016/j.ijrmms.2003.08.002.

Isler, A., Pasquier, F. & Huber, M. (1984): Geologische Karte der zentralen Nordschweiz 1:100'000. Herausgegeben von der Nagra und der Schweiz. Geol. Komm.

Jordan, P. (2016): Reorganisation of the Triassic stratigraphic nomenclature of northern Switzerland: overview and the new Dinkelberg, Kaiseraugst and Zeglingen formations. Swiss Journal of Geosciences, 109, 241-255.

Nagra (2014): SGT Etappe 2: Vorschlag weiter zu untersuchender geologischer Standortgebiete mit zugehörigen Standortarealen für die Oberflächenanlage. Geologische Grundlagen. Dossier II: Sedimentologische und tektonische Verhältnisse. Nagra Technischer Bericht NTB 14-02.

Pietsch, J. & Jordan, P. (2014): Digitales Höhenmodell Basis Quartär der Nordschweiz – Version 2013 (SGT E2) und ausgewählte Auswertungen. Nagra Arbeitsbericht NAB 14-02.

Plumb, R., Edwards, S., Pidcock, G., Lee, D. & Stacey, B. (2000): The Mechanical Earth Model concept and its application to high-risk well construction projects. SPE Paper #59128 presented at the IADC/SPE Drilling Conference, New Orleans, Louisiana, February 2000. DOI: https://doi.org/10.2118/59128-MS.

Wileveau, Y., Cornet, F.H., Desroches, J. & Blumling, P. (2007): Complete in situ stress determination in an argillite sedimentary formation. Physics and Chemistry of the Earth Parts A/B/C 32/8-14, 866-878. DOI: 10.1016/j.pce.2006.03.018.